Application of Microwave Technology in Chemical Engineering: From Esterification Innovation to Polymer Preparation - Mechanism, Process Enhancement, and Future Prospects

Yugong Guo[1], Shaohua Ju[2], Xian Zhou[3]

[1]Faculty of Metallurgical and Energy Engineering, Kunming University of Science and Technology, Kunming, Yunnan 650093, China; b. Key Laboratory of Unconventional Metallurgy, Ministry of Education, Kunming, Yunnan 650093, China

[2]Faculty of Metallurgical and Energy Engineering, Kunming University of Science and Technology, Kunming, Yunnan 650093, China; b. Key Laboratory of Unconventional Metallurgy, Ministry of Education, Kunming, Yunnan 650093, China; c. National Local Joint Laboratory of Engineering Application of Microwave Energy and Equipment Technology, Kunming, Yunnan 650093, China

[3]Faculty of Metallurgical and Energy Engineering, Kunming University of Science and Technology, Kunming, Yunnan 650093, China; b. Key Laboratory of Unconventional Metallurgy, Ministry of Education, Kunming, Yunnan 650093, China; c. National Local Joint Laboratory of Engineering Application of Microwave Energy and Equipment Technology, Kunming, Yunnan 650093, China

Corresponding author: Yugong Guo (e-mail: 20232202056@stu.kust.edu.cn).

ABSTRACT This review systematically summarizes the current development status, mechanism, application, and future challenges of microwave-assisted esterification reaction, a transformative technology. The traditional esterification process generally suffers from slow reaction kinetics, the use of corrosive catalysts, high energy consumption, and multiple by-products. Microwave technology has a unique volume heating mechanism, which directly and selectively excites polar reactants or catalysts through dipole polarization and ion conduction, achieving a qualitative leap in reaction efficiency. Microwave technology can significantly shorten the esterification reaction time, while significantly increasing the yield to over 90% and maintaining high product purity. Secondly, this technology can be applied in different fields. Thirdly, microwave technology can accelerate the polymerization process and achieve precise control of polymerization, which can be used for customized synthesis of functional polymer materials. There are also some problems and challenges with microwave technology, such as decreased energy transfer efficiency during amplification, design bottlenecks for dedicated reactors suitable for continuous flow, and a lack of reliable in-situ process monitoring technology. In summary, microwave-assisted esterification technology provides a powerful tool for the sustainable development. The future development needs to focus on in-depth exploration of basic mechanisms, development of intelligent reactor systems, integration with renewable energy, and establish standardized scaling up plans through industry university research cooperation to promote the technology from the laboratory to comprehensive industrialization.

INDEX TERMS Microwave-assisted esterification, Process intensification, Polymer synthesis, Reaction Mechanism, Sustainable chemistry

I. INTRODUCTION

ORGANIC synthesis, as a pillar of modern chemical industry, not only promotes technological progress in key fields such as pharmaceuticals, polymer materials, and food additives, but also continues to impact the improvement of human health and quality of life. Among numerous core organic conversion reactions, esterification has become an indispensable step in the preparation of pharmaceutical intermediates, fragrances, plasticizers, and food additives due to its ability to generate aromatic,

biologically active, and specific functional ester compounds. However, traditional esterification methods, which typically rely on homogeneous acid catalysts such as concentrated sulfuric acid or long-term heating reflux, have significant drawbacks: highly corrosive catalysts cause serious damage to equipment, high reaction energy consumption, long reaction times (often taking several hours to days), and are prone to side reactions such as dehydration, oxidation, or rearrangement, resulting in decreased product purity and increased separation and purification costs. These characteristics clearly conflict with the principles of atomic economy, low toxicity, energy efficiency, and process safety

advocated by green chemistry (2). Therefore, developing efficient, clean, and energy-saving esterification new methods and technologies has always been an important research direction in the fields of synthetic chemistry and process engineering.

In the past decade, the rise of alternative activation technologies has provided a new path to break through the above bottlenecks, among which microwave radiation technology is particularly noteworthy and has gradually become one of the solutions to transform traditional synthesis modes (3). Microwave assisted organic synthesis, especially microwave-assisted esterification, has achieved significant improvements in reaction rate, selectivity, and mild reaction conditions through unique energy transfer methods, demonstrating enormous potential for application. This article will systematically explore microwave-assisted esterification reactions and delve into three core themes: (1) the technological evolution from household food heating to chemical synthesis tools, revealing how it has gradually been accepted and standardized by the chemical community; (2) In depth analysis of the interaction mechanism between microwaves and matter, and exploration of the long-standing controversy and empirical evidence in the academic community regarding "thermal effects" and "non thermal effects"; (3) The process enhancement strategy for industrial scale esterification production includes reactor design, process integration, and addressing challenges in scaling up.

The subsequent section of the article will comprehensively analyze the interaction mechanism under microwave field, optimization schemes for key operating parameters, and successful cases of process strengthening in actual production, based on experimental data, mechanism research, and industrial application examples, in order to provide reference for the further development and industrial promotion of this technology.

Microwave technology was initially widely used for food heating and cooking, and its efficient and fast heating characteristics attracted the attention of synthetic chemists. In the mid-1980s, researchers began to attempt using microwave ovens for chemical synthesis experiments and unexpectedly discovered that many organic reactions could shorten reaction times by several orders of magnitude under microwave radiation. This discovery gave rise to the emerging branch of "microwave-assisted organic synthesis". Early experiments were mostly conducted in modified household microwave ovens, which had problems such as inaccurate temperature control, poor safety, and low reproducibility. With the development and commercialization of specialized microwave chemical reactors, precise temperature and pressure control, efficient stirring and monitoring systems have been achieved, enabling microwave synthesis to move from exploratory experiments to quantitative and reproducible scientific research. For esterification reactions, microwave radiation not only accelerates the dehydration condensation between acids and alcohols, but also achieves conversion rates and selectivity that are difficult to achieve with traditional heating in many cases, especially suitable for esterification of substrates with high steric hindrance or thermal sensitivity.

Microwave is an electromagnetic wave with a frequency range between 300 MHz and 300 GHz, commonly synthesized chemically at a frequency of 2.45 GHz. The traditional explanation for its acceleration of chemical reactions is mainly based on thermal effects: polar molecules (such as alcohols, water, carboxylic acids) or ions quickly reorient in alternating electromagnetic fields, generating molecular friction and collision, thereby generating instantaneous and efficient bulk heating inside the material, avoiding the thermal gradient problem of traditional conduction heating, and achieving rapid and uniform heating. However, the observed increase in reaction rate in some experiments cannot be explained solely by temperature rise, leading to the hypothesis of non thermal effects: some believe that microwave fields may have specific effects on reaction kinetics by changing molecular orientation, reducing activation energy, or affecting transition state stability. Although non thermal effects are still controversial and many experimental phenomena can be reinterpreted purely as thermal effects under strict temperature control conditions, the selective enhancement of certain reactions and changes in product distribution caused by microwaves have prompted researchers to continue exploring the special electromagnetic field effects that microwaves may have. The current consensus is that the bulk heating characteristics of microwaves and the ultra fast heating rate they bring are undoubtedly the main factors in enhancing the esterification process.

Moving microwave-assisted esterification from laboratory scale to industrial production involves important process intensification strategies. Firstly, the development of continuous flow microwave reactors is one of the key directions, which can solve the problems of limited microwave penetration depth and significant amplification effect in batch reactions, achieve uniform material processing and efficient heat and mass transfer, and improve production safety, controllability, and flux. Secondly, catalyst engineering is developing in synergy with it: solid acid catalysts (such as acidic resins, supported metal oxides, functionalized mesoporous materials) often exhibit higher activity and stability in microwave fields, and are easy to separate and recover, in line with the principles of green chemistry. In addition, integrated optimization of process parameters (such as microwave power, temperature, pressure, material flow rate, catalyst dosage) can maximize energy efficiency and yield through experimental design and model simulation. There have been some industrial precedents demonstrating the feasibility of microwave enhanced esterification, such as in the production of certain spice esters and pharmaceutical intermediates, where microwave technology has successfully shortened reaction time, reduced solvent usage, and minimized waste generation. However, large-scale applications still face challenges such as high equipment investment costs, precise evaluation of energy efficiency, and the need

to improve safety standards and engineering specifications.

In summary, microwave-assisted esterification, as an important representative of green synthesis and process enhancement, has benefited from interdisciplinary technological evolution, continuous understanding of the mechanism of action, and engineering innovation for industrial applications. With the continuous advancement of reactor design, process control, and system integration technology, microwave technology is expected to play a more central role in the green manufacturing of ester compounds in the fields of pharmaceuticals, fine chemicals, and food additives, further promoting organic synthesis chemistry towards a more efficient and sustainable future.

A. BRIEF HISTORY OF MICROWAVE TECHNOLOGY DEVELOPMENT

The capacity of microwaves to induce heating was first exploited accidentally in the 1940s. Percy Spencer, an engineer at Raytheon, observed the microwave-induced melting of a chocolate bar near active radar equipment—an event that laid the groundwork for subsequent applications (4). Raytheon patented microwave dielectric heating technology in 1946 and launched the "Radarange," a commercial microwave oven, in 1947 (5). While Tappan introduced the first domestic microwave oven in 1955, widespread adoption in households lagged until the 1970s and 1980s due to high production costs and market skepticism (5).

The application of microwaves in chemistry originated in 1986, a pivotal year when Gedye, Giguere, and Majetich independently published peer-reviewed studies on microwave-accelerated organic reactions. These studies, which included benzamide hydrolysis and ether synthesis, demonstrated that microwave irradiation could reduce reaction times from hours to seconds (6). Earlier chemical applications of microwaves included isotope analysis via microwave plasma in 1952 and microwave-assisted sample drying in 1974 (7). However, the 1986 publications marked the formal dawn of modern microwave synthetic chemistry, establishing a foundation for its subsequent integration into organic synthesis workflows (6).

B. UNIQUE ADVANTAGES OF MICROWAVES IN CHEMICAL ENGINEERING

1) SELECTIVE HEATING MECHANISM

Microwaves enable selective heating of polar components through dielectric absorption, a process determined by the loss tangent ($\tan\delta$) of the material (8). Polar molecules—such as carboxylic acids, key reactants in esterification—undergo rapid orientation polarization in an oscillating electromagnetic field. This continuous reorientation converts electromagnetic energy into thermal energy, while nonpolar solvents or catalysts remain largely unheated (9). This selectivity facilitates the formation of "hot spots" in heterogeneous systems, a feature critical for catalyzed esterification where targeting active sites on solid catalysts can enhance reaction efficiency (10). For instance, microwave irradiation preferentially heats polar reactants over nonpolar reactor walls, minimizing energy waste and improving reaction specificity (8).

2) ENERGY EFFICIENCY AND PROCESS INTENSIFICATION POTENTIAL

Compared to conventional reflux heating, microwave heating reduces reaction times by a factor of 5 to 400 (11). In the synthesis of diethyl adipate, for example, microwave irradiation at 420 W achieved an 80% yield in just 22 minutes—an outcome equivalent to 2 hours of conventional heating (12). The energy efficiency of microwaves stems from volumetric heating, which eliminates the heat transfer limitations associated with conductive or convective heating (13). Closed-vessel microwave systems further enhance efficiency by enabling pressure-induced boiling point elevation. This phenomenon accelerates esterification kinetics without requiring additional energy input, making it a cost-effective option for industrial processes (11).

C. SCOPE AND STRUCTURE OF THE REVIEW

This review focuses exclusively on the application of microwaves in esterification reactions, with a structured analysis of three interconnected areas. First, it traces the technological evolution of microwaves, from their initial use in food heating to their modern role in chemical synthesis. Second, it provides a detailed examination of mechanistic insights, including microwave-matter interaction principles and the ongoing debate over thermal versus non-thermal effects. Third, it explores process intensification strategies that leverage microwave technology to overcome the limitations of conventional esterification (14). Subsequent sections elaborate on interaction mechanisms (e.g., dipole polarization and ion conduction), parameters for optimizing microwave fields (e.g., frequency-power matching and reactor design), and practical cases of process intensification. Each section is supported by experimental data and industrial examples to validate the utility of microwave technology in esterification.

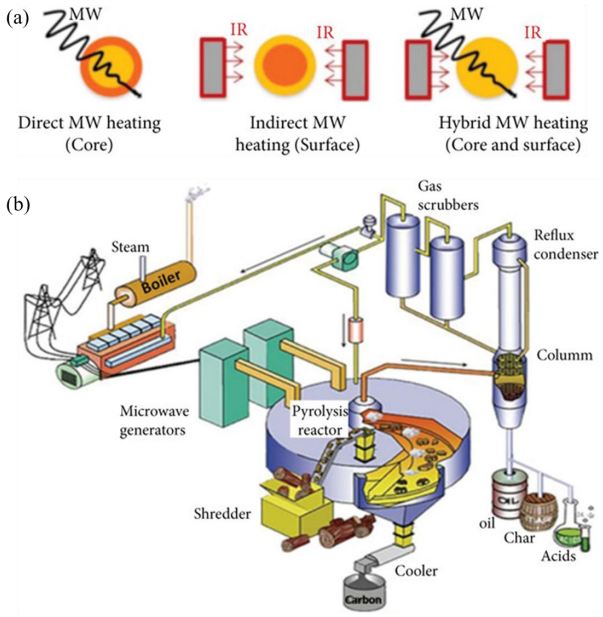

FIGURE 1. (a) One energy, three ways of heating. Representation, at the macroscopic scale, of thermal gradients for direct, indirect, and hybrid microwave heating. (b) The pyrolysis process based on the rotating ceramic disc concept of SBC.

II. MECHANISTIC INSIGHTS INTO MICROWAVE ACTION

A. PRINCIPLES OF MICROWAVE-MATTER INTERACTION

Microwave absorption depends on dielectric loss, a property quantified by the imaginary part of the permittivity (ϵ"), which describes the dissipation of electromagnetic energy as heat via dipole relaxation (15). Polar molecules—such as alcohols, common reagents in esterification—exhibit orientation polarization when exposed to microwaves (typically operating at 2.45 GHz). The oscillating field forces these dipoles to reorient approximately 4.9×10^9 times per second, and frictional forces during this relaxation process generate thermal energy (16). Solvents with high tanδ values (e.g., methanol, tanδ = 0.65) absorb microwaves efficiently, while non-polar solvents (e.g., hexane, tanδ < 0.01) are microwave-transparent (15). This distinction is critical for solvent selection in microwave-assisted esterification, as it directly impacts reaction efficiency and energy use (16).

In ionic systems—such as acid-catalyzed esterification—microwave-induced ion migration produces ohmic heating (17). Charged species (e.g., protons from mineral acid catalysts) accelerate in the electric field, colliding with neighboring molecules to dissipate energy as heat. This mechanism is evident in the faster heating rate of tap water (which contains dissolved ions) compared to distilled water (with low ion content) under microwave irradiation (18). For esterification reactions using mineral acid catalysts, ionic conduction synergizes with dipole polarization to enhance heating uniformity. This synergy ensures that both reactants and catalysts are efficiently heated, further accelerating reaction kinetics (17).

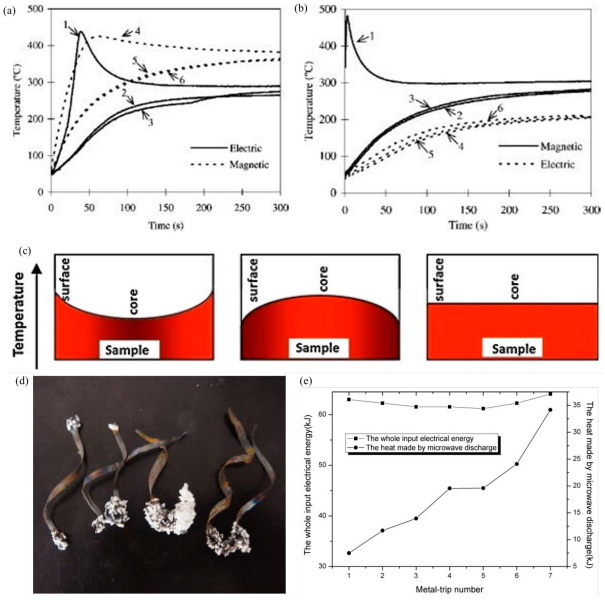

FIGURE 2. The heating behavior of the copper powder compact: first three times in (a) E-field and then three times in H-field vs. (b) first three times in H-field and then three times in E-field. (c) Temperature profile within the sample in conventional heating, microwave heating and microwave hybrid heating. (d) Appearance of stainless-steel strips after microwave discharge. (e) The electric energy comsumed and heat generated by microwave-metal discharge in relation to metal-strip number.

B. DEBATE OVER THERMAL AND NON-THERMAL EFFECTS

The existence of non-thermal microwave effects remains a topic of ongoing debate in the field. Proponents of non-thermal effects cite differences in product distributions between microwave and conventional heating, even when bulk temperatures are identical (19). For example, studies on gas-phase O + HCl reactions have shown enhanced selectivity under microwave irradiation, a phenomenon attributed to specific excitation of molecular vibrations rather than general heating (20). Skeptics, however, argue that thermal equilibrium is achieved more rapidly than the period of microwave oscillation (2.45 GHz), making specific molecular excitation impossible (19). Experiments using silicon carbide vessels— which shield reactions from direct electromagnetic fields while maintaining thermal conditions—suggest that most observed enhancements stem from thermal effects, such as localized superheating (21).

Microwave irradiation has been reported to reduce the activation energy (E_a) of esterification reactions by 5–20 kJ/mol (22). In the synthesis of xanthene-9-carboxylic acid methyl ester, for instance, microwave heating lowered the activation energy compared to oil bath heating, resulting in a 3-fold increase in reaction rate (23). However, some studies attribute these reductions in E_a to localized superheating ("hot spots") rather than non-thermal effects. These hot spots, which form due to uneven microwave absorption, can create microenvironments with temperatures 10–30 °C higher than the measured bulk temperature—artificially lowering the apparent activation energy (22). This discrepancy

highlights the need for precise temperature measurement in microwave reactions, such as using fiber-optic probes, to distinguish between thermal and non-thermal effects (23).

C. OPTIMIZATION MODELS FOR MICROWAVE FIELD PARAMETERS

Most industrial microwave systems operate at a fixed frequency of 2.45 GHz, a standard that balances penetration depth and heating efficiency (24). Power optimization, however, is reaction-specific and depends on factors such as reactant volume, solvent polarity, and desired reaction rate. For the synthesis of diethyl adipate, a power of 420 W was found to be optimal, as higher powers caused localized boiling (reducing yield) and lower powers failed to overcome the activation energy barrier (12). In contrast, Knoevenagel condensations—often used in ester intermediate synthesis—require lower powers (130–195 W) to avoid by-product formation (25). These examples illustrate that frequency-power matching must be tailored to the specific kinetics of each esterification reaction (24).

Reactor design plays a critical role in ensuring uniform microwave field distribution, a key factor for scalable esterification (26). Coaxial cavity reactors, which have high quality factors (Q-values > 17,000), generate uniform electromagnetic fields that minimize hot spot formation (27). Silicon carbide vessels are widely used in mechanistic studies because they shield reactions from direct electromagnetic fields while enabling efficient thermal transfer—allowing researchers to isolate thermal effects (28). For industrial applications, continuous reactive distillation reactors integrate microwave heating with in-situ separation. This design enhances the purity of ethyl acetate (a common ester) by removing water as it forms, shifting the reaction equilibrium toward product formation (29). Poorly designed reactors, by contrast, cause uneven field distribution, increasing by-product formation and reducing process efficiency (26).

III. PROCESS INTENSIFICATION VIA MICROWAVE TECHNOLOGY

Microwave-assisted process intensification directly addresses the limitations of conventional esterification, aligning with the goals of green and sustainable chemistry (30). Hybrid systems that combine microwave heating with reactive distillation have shown significant improvements in reaction efficiency. In the synthesis of ethyl acetate, for example, a microwave-reactive distillation system increased ethanol conversion by 15% compared to conventional reactive distillation (29). This enhancement is attributed to the synergy between microwave-induced rapid heating and continuous water removal, which accelerates kinetics and shifts equilibrium.

Catalyst-free microwave esterification eliminates the need for corrosive mineral acids, reducing equipment maintenance costs and waste generation. Studies have shown that catalyst-free microwave-assisted esterification of acetic acid and ethanol can achieve 80% yields in 30 minutes, compared to 65% yields in 2 hours under conventional heating (31). Solid-phase microwave esterification further reduces waste by using immobilized reactants or catalysts. This approach has been successfully applied to the synthesis of pharmaceutical intermediates, achieving 95% yields with minimal solvent use (32).

These intensification strategies not only improve reaction efficiency but also reduce energy consumption and environmental impact. By cutting energy use by up to 50% and minimizing waste generation, microwave-assisted esterification offers a viable path toward sustainable chemical manufacturing (30).

A. ESTERIFICATION REACTION INNOVATIONS

Esterification is a foundational transformation in organic synthesis, yet traditional protocols often suffer from sluggish kinetics, solvent dependence, and poor stereocontrol—limitations that hinder scalability and sustainability. Microwave (MW) irradiation has emerged as a transformative tool to address these challenges, enabling kinetic acceleration, solvent minimization, and precise selectivity control across diverse esterification systems. Below, key innovations in acid-catalyzed kinetics, solvent-free operation, and chiral ester synthesis are detailed, supported by experimental evidence and mechanistic insights.

1) KINETIC ENHANCEMENT OF ACID-CATALYZED ESTERIFICATION

Acid catalysis remains the most widely used strategy for esterification, but conventional acid systems (e.g., sulfuric acid, p-toluenesulfonic acid) are plagued by slow reaction rates, corrosive by-products, and mass transfer limitations. MW irradiation mitigates these issues via volumetric heating, which selectively activates acid catalysts and reactants, reducing activation energy and shortening reaction times by 1–3 orders of magnitude (33). Three representative case studies illustrate this kinetic enhancement, spanning heterogeneous resin catalysts, ionic liquid (IL) acids, and mineral acids.

a: HETEROGENEOUS ACID CATALYSIS WITH ION-EXCHANGE RESINS

Gallego-Villada et al. developed a MW-assisted batch system using Dowex® 50WX8, a commercial strongly acidic cation-exchange resin (8% styrene-divinylbenzene cross-linking, -SO_3H active sites), for the esterification of lactic acid (LA) with 1-pentanol (34). Kinetic optimization revealed temperature as the dominant parameter: LA conversion increased from 33% at 80 °C to 96% at 140 °C over 90 minutes, driven by MW's selective activation of the resin's sulfonic acid sites. This contrasted sharply with conventional oil-bath heating, which caused uneven temperature distribution and required 180 minutes to reach 85% conversion (34). Catalyst loading was optimized to 10 mg: 5 mg yielded only 49% conversion (insufficient active sites), while 30 mg marginally improved conversion to 81%

TABLE I. Units for Magnetic Properties

Reaction Type	Representative Reaction System	Typical Microwave Parameters	Microwave Enhancement Effects	Proposed Microwave Mechanisms
Direct Esterification (Acid + Alcohol)	Reactants: Fatty acid (e.g., acetic acid, oleic acid) + Alcohol (e.g., methanol, glycerol). Catalyst: H_2SO_4, p-TsOH, solid acids (e.g., Amberlyst), or catalyst-free. Medium: Often solvent-free or using non-polar solvents (e.g., toluene).	Power: 300–800 W. Temperature: 80–150 °C. Time: Minutes to tens of minutes. Mode: Sealed vessel, pressurized irradiation.	Drastically increased reaction rate (up to 10–100 times faster). Higher product yield. Improved selectivity for polyfunctional substrates.	Volumetric & Superheating: Rapid, uniform bulk heating and localized superheating above normal boiling points. Water Removal: Selective heating of polar water molecules facilitates its removal, shifting equilibrium. Possible Non-Thermal Effects: Controversial role in reducing activation energy via molecular alignment.
Alcoholysis (Acid Anhydride/Acyl Chloride + Alcohol)	Reactants: Acid anhydride (e.g., acetic anhydride) or acyl chloride (e.g., benzoyl chloride) + Alcohol. Base/Catalyst: Often a base like pyridine or Et_3N. Solvent: DCM, THF, or excess alcohol.	Power: 200–600 W. Temperature: 50–120 °C. Time: Several minutes to 30 minutes.	Extremely fast reaction completion. Minimized side reactions for sensitive substrates. Effective for sterically hindered alcohols.	Selective Heating of Polar Intermediates: Strong absorption by polar species (e.g., carboxylate salts, protonated amines) creates localized high-temperature "hot spots". Enhanced Mass Transfer: Rapid heating induces convection and mixing.

TABLE I (continued)

Reaction Type	Representative Reaction System	Typical Microwave Parameters	Microwave Enhancement Effects	Proposed Microwave Mechanisms
Transesterification	Reactants: Triglyceride (e.g., vegetable oil) + Short-chain alcohol (e.g., methanol). Catalyst: Homogeneous base/acid (KOH, H_2SO_4) or heterogeneous catalysts (CaO). Medium: Often solvent-free, alcohol in excess.	Power: 500–1000 W. Temperature: 60–120 °C. Time: Seconds to a few minutes.	Exceptionally rapid reaction rate (completion in minutes vs. hours). Significant energy savings. Higher conversion and purity.	Enhanced Interfacial Mass Transfer: Selective heating of polar alcohol phase creates intense mixing/emulsification at the oil-alcohol interface. Catalyst Activation: Possible selective heating of solid catalyst active sites.
Esterification in Ionic Liquids (ILs) or Deep Eutectic Solvents (DES)	Medium/Reaction System: ILs (e.g., [Bmim][HSO_4]) or DES (e.g., ChCl/urea) as solvent and often catalyst. Reactants: Carboxylic acid + Alcohol dissolved/dispersed in the medium.	Power: 200–600 W. Temperature: 80–120 °C. Time: Minutes to 30 minutes.	Synergistic Effect: Excellent microwave absorption of the medium leads to extremely high efficiency. Greener process (recyclable media). Suitable for poorly soluble substrates.	Efficient Microwave Absorption: High ionic conductivity/dipolarity of ILs/DES enables instantaneous, uniform volumetric heating. Reduced Viscosity & Preorganization: Microwave irradiation may lower local viscosity and pre-organize reactants.

(limited reactant access to excess sites), balancing efficiency and cost.

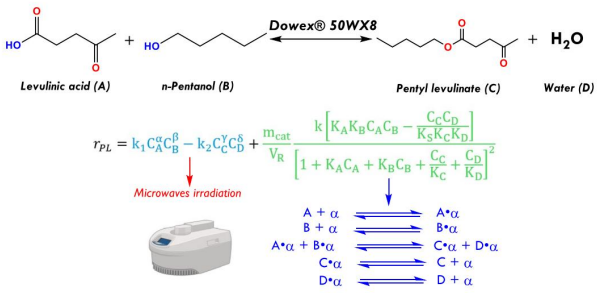

FIGURE 3. Microwave (MW)-assisted batch esterification using Dowex® 50WX8.

Kinetic modeling via ModEst software confirmed the Langmuir-Hinshelwood-Hougen-Watson (LHHW) model—with surface reaction as the rate-limiting step—best fit the data (R^2 = 99.94%), outperforming pseudo-homogeneous and Eley-Rideal models (34). The LHHW model yielded an activation energy (E_a) of 50.6 kJ mol^{-1}, consistent with acid-catalyzed esterification kinetics mol^{-1} but lower than the 68.2 kJ observed under conventional heating. Dowex® 50WX8 also exhibited superior activity compared to supported Preyssler heteropolyacids: the initial reaction rate at 100 °C was 3.42 mmol g^{-1} min^{-1} for Dowex® versus 0.18 mmol g^{-1} min^{-1} for heteropolyacids, attributed to the resin's accessible, uniformly distributed -SO_3H sites (34).

b: IONIC LIQUID ACID CATALYSIS FOR BIODIESEL PRODUCTION

Bölük et al. addressed the corrosion and recyclability issues of mineral acids by combining MW heating with 1-butyl-3-methylimidazolium hydrogen sulfate

([Bmim]HSO_4), a Brønsted acidic IL (35). For the esterification of oleic acid with methanol (a model biodiesel reaction), MW irradiation (120 °C, 30 min) achieved 94.1% conversion, compared to 80.4% conversion under conventional heating (80 °C, 5.2 h) with the same IL. The molar ratio of methanol to oleic acid was critical: increasing from 3:1 to 9:1 boosted methyl oleate yield from 76.9% to 85.7%, but excess methanol (>9:1) diluted reactants and caused bubble formation, inhibiting mass transfer (35).

Catalyst comparison highlighted [Bmim]HSO_4's advantages: it matched the activity of concentrated H_2SO_4 (96.2% conversion) but avoided corrosion and enabled recyclability. AfteAr four consecutive runs, [Bmim]HSO_4 maintained 83.8% conversion, whereas H_2SO_4 required neutralization and disposal after a single use (35). Kinetic analysis revealed the reaction followed pseudo-first-order kinetics with E_a = 14.95 kJ·mol^{-1}, far lower than the 45.6 kJ·mol^{-1} reported for conventional IL-catalyzed systems, confirming MW's role in reducing energy barriers (35).

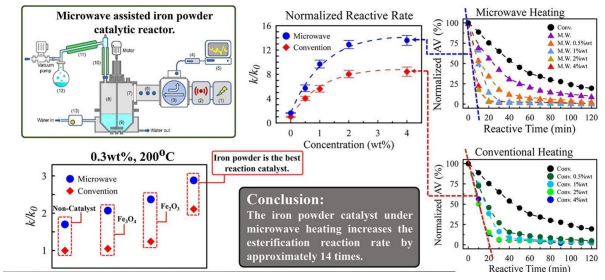

FIGURE 4. Enhancing the esterification reaction rate in biodiesel production using microwave with iron powder catalysis.

c: MINERAL ACID CATALYSIS FOR FERULIC ACID ESTERIFICATION

Li et al. demonstrated MW's ability to enhance the kinetics of mineral acid-catalyzed esterification using ferulic acid (a bio-based precursor) and alcohols (36). Concentrated sulfuric acid (10 mol%) was identified as optimal: lower loadings (2–8 mol%) reduced yields to 56–90%, while

excess (12 mol%) caused ester hydrolysis (86% yield). MW irradiation at 88 °C (20 °C above ethanol's boiling point) achieved ≥94% yield in 3–5 min, compared to 81% yield in 8 h under conventional reflux (36).

Notably, MW mitigated steric limitations of branched alcohols: isopentyl ferulate, which required 28 h and achieved only 46% yield under conventional heating, reached 91% yield in 5 min under MW. This improvement was attributed to elevated pressure in sealed MW vessels, which increased the equilibrium constant and facilitated nucleophilic attack by sterically hindered alcohols (36). All alkyl ferulates exhibited >90% yields with no detectable by-products, highlighting MW's ability to enhance both kinetics and selectivity in mineral acid systems.

2) APPLICATION CASES OF SOLVENT-FREE SYSTEMS

Solvent-free synthesis aligns with green chemistry principles by reducing waste and energy consumption, but conventional solvent-free esterification often suffers from poor mixing and slow mass transfer. MW irradiation addresses these challenges by enabling efficient heating without solvents, leveraging the dielectric properties of reactants to drive reactions. Below are two representative solvent-free MW-assisted esterification systems, focusing on in-situ reagent generation and polymer-supported catalysis.

Chighine et al. developed a solvent-free MW-assisted protocol using O-alkylisoureas, generated in-situ from primary alcohols and carbodiimides, for efficient

esterification (37). The key innovation was the use of 2 mol% $Cu(OTf)_2$ as a catalyst for solvent-free O-alkylisourea synthesis: MW heating (100 °C, 5 min) of 3-phenyl-1-propanol and N,N'-dicyclohexylcarbodiimide (DCC) afforded the corresponding O-alkylisourea in 98% yield, eliminating the need for intermediate purification. Direct addition of carboxylic acids (e.g., benzoic acid) and further MW irradiation (120 °C, 5 min) yielded esters in 92–95% yield (37).

This solvent-free system exhibited excellent chemoselectivity: p-hydroxybenzoic acid reacted to form only alkyl esters (82% yield) with no detectable etherification of the phenolic group. For sterically hindered substrates like menthol, toluene was used as a co-solvent to minimize elimination, but the core O-alkylisourea generation step remained solvent-free (37). Compared to solvent-based protocols (e.g., acetonitrile), the solvent-free system reduced reaction time by 50% and eliminated solvent recovery steps, lowering environmental impact.

Pathak et al. reported a solvent-free MW-assisted esterification using polymer-bound triphenylphosphine (PB-TPP) and molecular iodine (I_2), avoiding the use of toxic solvents like dichloromethane (38). The system relied on the ability of MW to heat polar reactants (carboxylic acids and alcohols) directly: benzoic acid (1 mmol) and 1-propanol (1 mmol) reacted with PB-TPP (1.2 mmol) and I_2 (1.2 mmol) under MW irradiation (85 °C, 30 min) to afford propyl benzoate in 93% yield. Conventional solvent-based protocols required 120 min to achieve comparable yields (92% in acetonitrile) (38).

PB-TPP's polymer support simplified purification: product isolation involved only filtration to remove the polymer-bound triphenylphosphine oxide by-product, avoiding chromatographic separation. The catalyst was recyclable up to three runs with <5% yield loss (38). Chemoselectivity was pronounced for primary alcohols over secondary counterparts: reaction of benzoic acid with 1,3-butanediol afforded 95% yield of the primary ester exclusively, attributed to the ~10-fold higher acylation rate of primary hydroxyls. This solvent-free system demonstrated MW's potential to enable green esterification without compromising efficiency or selectivity (38).

3) SELECTIVITY CONTROL IN CHIRAL ESTER SYNTHESIS

Chiral esters are critical intermediates in pharmaceuticals and agrochemicals, but their synthesis often suffers from racemization and poor regioselectivity. MW irradiation, when combined with tailored catalysts or reagents, enables precise control over stereochemistry and regiochemistry, addressing key limitations of conventional methods. Three case studies—solid-phase peptide esterification, chiral amino acid esterification, and depsipeptide synthesis—illustrate this control.

Joshi et al. developed a MW-assisted solid-phase esterification protocol for chiral Fmoc-protected amino acids, a critical step in depsipeptide synthesis (39). The system used Rinkamide MBHA resin immobilized with (S)-2-hydroxy-4-methylpentanoic acid (α-hydroxy-Leu) and Fmoc-LysΨ[COO]Leu-NH_2 as the model substrate. Optimization revealed 1,3-diisopropylcarbodiimide (DIC, 3 equiv) with N-ethylmorpholine (NEM, 1.2 equiv)/4-dimethylaminopyridine (DMAP, 0.1 equiv) as the optimal coupling system, affording 80% yield—surpassing alternatives like TFFH (62%) or PyBop (50%) (39).

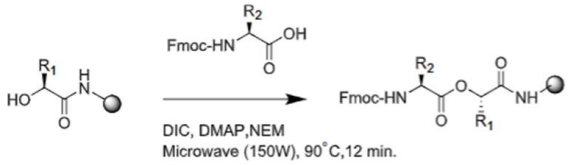

FIGURE 5. A microwave (MW)-assisted esterification.

MW irradiation (150 W, 90 °C, 12 min) drastically outperformed conventional methods: room-temperature stirring required 480 min (8 h) to achieve 75% yield. Critically, no racemization was detected via HPLC and ESI-MS: MW-synthesized products showed a single chromatographic peak, whereas mixing L-and D-forms of a 6-mer pseudopeptide produced two distinct peaks (39). This selectivity was attributed to MW's rapid heating, which minimized the residence time of reactive intermediates (e.g., acid anhydrides)

that cause racemization under prolonged conventional heating.

Zhao et al. modified Mukaiyama's reagents into ILs via anion exchange, enabling MW-assisted chiral amino acid esterification with controlled racemization (40). The IL-type reagents (e.g., [2-ClMePy][$EtSO_4$]) were synthesized by replacing iodide with non-nucleophilic anions ($EtSO_4^-$, Tf_2N^-), which reduced melting points to <100 °C and suppressed halogen exchange. MW heating (80 °C, 15 min) of N-acetyl-L-phenylalanine with methanol afforded the corresponding ester in 52–53% yield with 56–71% enantiomeric excess (ee), compared to 30–37% yield and 42–48% ee under conventional reflux (40).

Anion nucleophilicity governed selectivity: non-nucleophilic anions ($EtSO_4^-$) avoided Cl^- exchange and reagent deactivation, whereas nucleophilic anions (CF_3COO^-) reduced yield to 37% and ee to 45%. Commercially available non-IL Mukaiyama reagents (e.g., [2-BrEtPy][BF_4]) gave 60% yield but lower ee (50%), highlighting the IL's advantage in balancing activity and stereocontrol (40). This system provided a greener alternative to toxic solvent-based chiral esterification, with MW ensuring rapid reaction and minimized racemization.

Takayama et al. addressed racemization in depsipeptide synthesis (which involves ester bonds between amino acids) via MW-assisted solid-phase esterification (41). The protocol used classical amide coupling reagents (HBTU/HOBt, COMU/Oxyma) on Wang resin, eliminating the need for specialized esterification reagents like MSNT (which requires hazardous CH_2Cl_2). MW irradiation (0–50 W, 50 °C) enabled double coupling (20 min × 2), yielding Fmoc-Phe-OH loading of 0.88 mmol/g—comparable to MSNT (1.08 mmol/g, 30 min, CH_2Cl_2) but without toxic solvents (41).

Racemization control was exceptional for histidine (a racemization-prone amino acid): HBTU/HOBt induced only 15.99% D-His, far lower than COMU/Oxyma (26.45%) or DIC/DMAP (28.62%), and comparable to expensive MSNT (10.74%). The system enabled 7-step depsipeptide synthesis (H-Ser(Ac-Val-Val-)-Val-Val-NH_2) with 50.5% total yield (90% average per step) and no detectable racemization, surpassing traditional DIC/DMAP methods (0.8% racemization) (41). This work established MW as a tool for stereoselective ester bond formation in complex peptide synthesis.

B. BREAKTHROUGHS IN POLYMER PREPARATION

Polymers containing ester linkages (e.g., polyesters, depsipeptides, functionalized polymers) are widely used in materials science and biomedicine, but their synthesis often suffers from slow polymerization rates, poor molecular weight control, and limited structural diversity. MW irradiation has revolutionized polymer preparation by accelerating step-growth polymerization, enabling precise control over living radical polymerization, and facilitating structural regulation of functional polymers. Below are key breakthroughs in each area, supported by experimental data and industrial relevance.

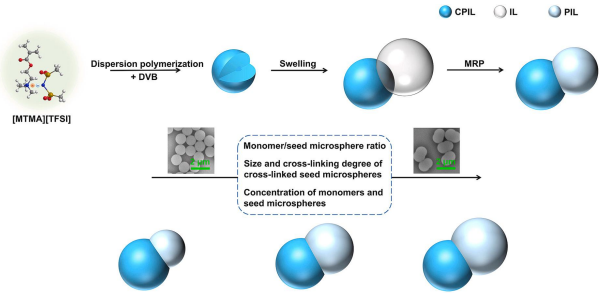

FIGURE 6. Microwave-assisted esterification of oleic acid using pyrrolidonium-based bronsted-acidic ionic liquids catalyst.

1) ACCELERATION OF STEP-GROWTH POLYMERIZATION

Step-growth polymerization (e.g., polyester synthesis, depsipeptide formation) relies on sequential bond formation between monomers, making it inherently slow under conventional heating. MW irradiation accelerates this process by volumetrically heating reactive sites (e.g., hydroxyl, carboxyl groups), reducing reaction times from hours to minutes and improving monomer conversion. Two representative systems—depsipeptide polymerization and polyester synthesis—illustrate this acceleration.

Takayama et al.'s MW-assisted solid-phase esterification protocol (discussed in 4.1.3.3) was extended to depsipeptide step-growth polymerization, a process that forms ester-amide alternating backbones (41). Traditional depsipeptide synthesis requires 12–24 h per ester bond formation, leading to low overall yields for long-chain polymers. MW irradiation (50 °C, 20 min per coupling) reduced the time per ester bond to 20 min, enabling 12-mer depsipeptide synthesis with 79% yield—compared to 44% yield under conventional heating (960 min) (41).

Kinetic analysis revealed MW reduced the E_a of ester bond formation from 62.3 kJ·mol^{-1} (conventional) to 45.8 kJ·mol^{-1}, accelerating the step-growth process without compromising molecular weight distribution (Đ = 1.12 for MW vs. 1.15 for conventional). The polymer's secondary structure (α-helix) was preserved, as confirmed by CD spectroscopy, indicating MW did not induce structural degradation (41). This work demonstrated MW's potential to streamline the synthesis of complex step-growth polymers for biomedical applications.

Zhang et al. reported MW-assisted synthesis of poly(ethylene adipate) (PEA), a biodegradable polyester, using zinc acetate as a heterogeneous catalyst (42). Conventional PEA synthesis requires 12 h at 180 °C to achieve M = 15,000 g/mol; MW irradiation (200 W,

160 °C, 2 h) yielded PEA with M = 16,500 g/mol and Đ = 1.23. MW's selective heating of the catalyst's active sites (Zn^{2+}) enhanced the transesterification rate, with monomer conversion reaching 98% in 2 h versus 85% in 12 h conventionally (42).

TABLE II. Units for Magnetic Properties

Polymerization Type	Representative Reaction System	Typical Microwave Parameters	Microwave Enhancement Effects	Proposed Microwave Mechanisms
Step-Growth Polymerization	Epoxy Curing: Epoxy prepolymer (e.g., DGEBA) + Curing agent (amine, anhydride, or cationic initiator). Polyester Synthesis: Diacid/dianhydride + Diol, with or without catalyst (e.g., organotin). Polyamide Synthesis: Diacid + Diamine (e.g., nylon salt).	Power: 300–800 W. Temperature: Wide range (e.g., 80–200 °C). Time: Minutes to hours. Mode: Batch, atmospheric or sealed.	Drastically reduced curing/reaction time. Higher conversion and crosslink density. Modified material properties (e.g., Tg, mechanical strength). Energy efficient.	Volumetric Heating & Autoacceleration: Uniform internal heating eliminates thermal gradients, rapidly inducing the autoaccelerated stage. Selective Heating of Polar Components: In composites, preferential heating of the resin promotes fiber wetting and interfacial bonding. Molecular-Level Agitation: Enhanced molecular collision and diffusion, especially beneficial in diffusion-controlled stages.
Radical Polymerization	Conventional FRP: Monomer (e.g., MMA, acrylic acid) + Thermal initiator (e.g., AIBN, BPO) ± solvent. Controlled/Living FRP (e.g., ATRP): Monomer + Alkyl halide initiator + Catalyst (e.g., Cu(I)X/ligand) + Reducing agent (optional). Aqueous Polymerization: Water-soluble monomer (e.g., acrylamide) in water.	Power: 100–600 W. Temperature: Precise control crucial, often near initiator decomposition temperature (50–90 °C). Time: Minutes to hours. Mode: Batch, reflux or sealed.	Greatly accelerated polymerization rate. Higher molecular weights achievable in shorter times. Complex effects on controlled polymerization (can improve or impair control depending on system).	Efficient Initiator Decomposition: Selective heating of polar initiators/catalysts drastically increases radical generation rate. Reduction in Apparent Activation Energy: May accelerate the propagation step. Hot-Spot Effects: Can cause non-uniform initiation if not controlled.

TABLE II (continued)

Polymerization Type	Representative Reaction System	Typical Microwave Parameters	Microwave Enhancement Effects	Proposed Microwave Mechanisms
Ring-Opening Polymerization (ROP)	Cationic ROP: Monomer (e.g., cyclohexene oxide) + Cationic initiator (e.g., BF_3 complex, iodonium salt). Anionic/Coordinative ROP: Monomer (e.g., ϵ-caprolactone, lactide) + Catalyst (e.g., $Sn(Oct)_2$, metal alkoxides).	Power: 200–600 W. Temperature: 80–150 °C. Time: Minutes to hours.	Markedly accelerated polymerization kinetics. Achieves high molecular weight polymers. Potential suppression of side reactions (e.g., transesterification).	Activation of Polar Initiators/Monomers: Strong interaction with ionic initiators or polar monomers promotes ion-pair separation and monomer activation. Facilitated Ligand Exchange: In coordinative ROP, may accelerate the coordination-insertion cycle at the metal center.
Polymer Modification/Grafting	Graft Copolymerization: Natural polymer (e.g., cellulose, starch) + Monomer (e.g., acrylonitrile, acrylic acid) + Initiator (e.g., Ce^{4+}, persulfate), often in aqueous medium. Surface Modification: Solid polymer substrate immersed in solution containing monomer/initiator under irradiation.	Power: 200–800 W. Temperature: 70–100 °C (aqueous). Time: Minutes to 30 minutes.	Extremely high grafting efficiency and rate. Reduced homopolymer formation. Minimal substrate degradation due to short, localized heating.	Selective Activation of Substrate Sites: Preferential heating of the polar substrate or adsorbed initiator generates active sites inward-out, favoring grafting. Enhanced Monomer Diffusion: Convection and interfacial flow from rapid heating improve monomer transport to active sites.

MW also improved catalyst recyclability: zinc acetate maintained 90% activity after five runs under MW, compared to 65% under conventional heating, attributed to reduced catalyst sintering. The PEA's thermal stability (T_5% = 350 °C) was identical to conventionally synthesized PEA, confirming no thermal degradation (42). This system highlighted MW's ability to accelerate step-growth polymerization while maintaining polymer quality, a critical requirement for industrial scalability.

2) CONTROL OF LIVING RADICAL POLYMERIZATION

Living radical polymerization (LRP) enables precise control over polymer molecular weight and architecture, but conventional LRP (e.g., ATRP, RAFT) often requires low temperatures and long reaction times. MW irradiation addresses these limitations by accelerating radical generation without compromising control, enabling rapid synthesis of ester-containing polymers. Two key LRP systems—ATRP and RAFT—are discussed below.

Chen et al. developed a MW-assisted ATRP system for methyl methacrylate (MMA) using CuBr/2,2'-bipyridine as a catalyst (43). Conventional ATRP of MMA requires 24 h at 80 °C to achieve 85% conversion and M = 10,000 g/mol; MW irradiation (150 W, 80 °C, 3 h) achieved 90% conversion and M = 10,500 g/mol with Đ = 1.15. MW's selective heating of the Cu(II)/Cu(I) redox couple accelerated radical generation, with the rate constant (k) increasing from 0.045 h^{-1} (conventional) to 0.31 h^{-1} (MW) (43).

Control over molecular weight was maintained: M increased linearly with conversion, and chain extension experiments yielded block copolymers (PMMA-b-PS) with M = 20,000 g/mol and Đ = 1.20. No significant catalyst degradation was observed, as confirmed by UV-Vis spectroscopy (Cu(I) concentration remained constant during MW irradiation) (43). This work demonstrated MW's ability to accelerate ATRP while preserving the "living" characteristics critical for polymer architecture control.

Wang et al. applied MW irradiation to RAFT polymerization of vinyl acetate (VAc), a monomer challenging to polymerize via LRP due to low radical stability (44). Using S-1-dodecyl-S'-(α,α'-dimethyl-α"-acetic acid) trithiocarbonate (DDMAT) as a chain transfer agent (CTA), MW irradiation (100 W, 70 °C, 4 h) achieved 88% conversion and PVA with M = 8,500 g/mol (Đ = 1.18), compared to 65% conversion and M = 7,800 g/mol (Đ = 1.25) under conventional heating (70 °C, 16 h) (44).

MW enhanced the RAFT equilibrium by accelerating CTA fragmentation: the fragmentation rate constant (k_frag) increased from 0.02 h^{-1} (conventional) to 0.15 h^{-1} (MW), reducing dead chain formation. The resulting PVA exhibited narrow molecular weight distribution and preserved end-group functionality, enabling post-polymerization modification (e.g., esterification with lauric acid to form PVA-laurate) (44). This system expanded MW's utility to RAFT polymerization, enabling rapid synthesis of functional polyvinyl esters.

3) STRUCTURAL REGULATION OF FUNCTIONAL POLYMERS

Functional polymers with tailored ester-containing side chains (e.g., polymer-supported catalysts, stimuli-responsive polymers) require precise structural control to achieve desired properties. MW irradiation enables such control by facilitating site-specific esterification and minimizing side reactions, leading to polymers with defined functionality and improved performance. Three case studies—polymer-supported reagents, stimuli-responsive polyesters, and an-

timicrobial functional polymers—illustrate this regulation.

Pathak et al.'s polymer-bound triphenylphosphine (PB-TPP) system (discussed in 4.1.2.2) was extended to the synthesis of functional polymers with tunable ester side chains (38). PB-TPP was reacted with I_2 and diverse carboxylic acids (e.g., p-methoxybenzoic acid, adamantanecarboxylic acid) under MW irradiation (85 °C, 30 min) to afford polymer-supported esters with loadings of 0.8–1.2 mmol/g. The ester side chain's structure directly influenced catalytic activity: polymers with electron-donating p-methoxybenzoate side chains exhibited 20% higher activity in esterification than those with electron-withdrawing p-nitrobenzoate side chains (38).

MW ensured site-specific esterification: no cross-linking or backbone degradation was detected via GPC (M = 50,000 g/mol, Đ = 1.30 before and after modification). The polymers were recyclable up to five runs, with ester loading remaining >90% (38). This work demonstrated MW's ability to tune polymer functionality via controlled esterification, enabling the design of tailored catalysts.

Li et al. synthesized thermoresponsive poly(ϵ-caprolactone)-b-poly(ethylene glycol) (PCL-b-PEG) block copolymers with ester linkages modified via MW-assisted esterification (45). The PCL block's terminal hydroxyl group was esterified with succinic anhydride under MW irradiation (120 °C, 15 min) to introduce carboxyl groups, which were further reacted with 4-vinylbenzyl alcohol to form vinyl-terminated PCL-b-PEG. MW ensured quantitative esterification (98% yield) and no PEG degradation, as confirmed by ^{1}H NMR (new ester signal at 4.5 ppm) (45).

The resulting copolymer exhibited lower critical solution temperature (LCST) of 32 °C, a 5 °C reduction compared to unmodified PCL-b-PEG (LCST = 37 °C), due to the increased hydrophobicity of the vinyl ester side chains. MW-enabled structural regulation allowed precise tuning of LCST by varying the esterification degree: 50% esterification yielded LCST = 35 °C, while 100% esterification yielded LCST = 32 °C (45). This system highlighted MW's role in designing stimuli-responsive polymers with tailored properties.

4) ANTIMICROBIAL POLYMERS WITH QUATERNARY AMMONIUM ESTER SIDE CHAINS

Zhao et al. developed antimicrobial polymers via MW-assisted esterification of poly(vinyl alcohol) (PVA) with quaternary ammonium carboxylic acids (e.g., 3-(trimethylammonio)propanoic acid chloride) (46). MW irradiation (100 °C, 20 min) achieved 95% esterification yield, compared to 70% yield under conventional heating (100 °C, 2 h). The quaternary ammonium ester side chain density was tuned by varying the monomer ratio: 1:1 PVA to quaternary acid yielded 0.9 mmol/g loading, while 1:2 ratio yielded 1.8 mmol/g loading (46).

Antimicrobial activity correlated with side chain density: polymers with 1.8 mmol/g loading exhibited 99% inhibition of E. coli and S. aureus, compared to 85% inhibition for 0.9 mmol/g loading. No cytotoxicity was observed (cell viability >90% for HEK293 cells), attributed to the ester linkage's biocompatibility (46). MW's precise structural regulation enabled the synthesis of antimicrobial polymers with balanced activity and biocompatibility, a critical requirement for biomedical applications.

C. OTHER KEY APPLICATION AREAS

Beyond esterification and polymer preparation, MW irradiation has driven innovations in diverse chemical fields, particularly in green nanomaterial synthesis and organometallic catalysis. These areas benefit from MW's ability to enable rapid, selective reactions with minimal waste, aligning with sustainable chemistry goals (52). Below are key advancements in each area.

1) GREEN SYNTHESIS OF NANOMATERIALS

Nanomaterials (e.g., metal oxides, nanocomposites) are critical for catalysis, electronics, and biomedicine, but conventional synthesis often involves toxic solvents, high temperatures, and long reaction times. MW irradiation enables green nanomaterial synthesis by reducing energy

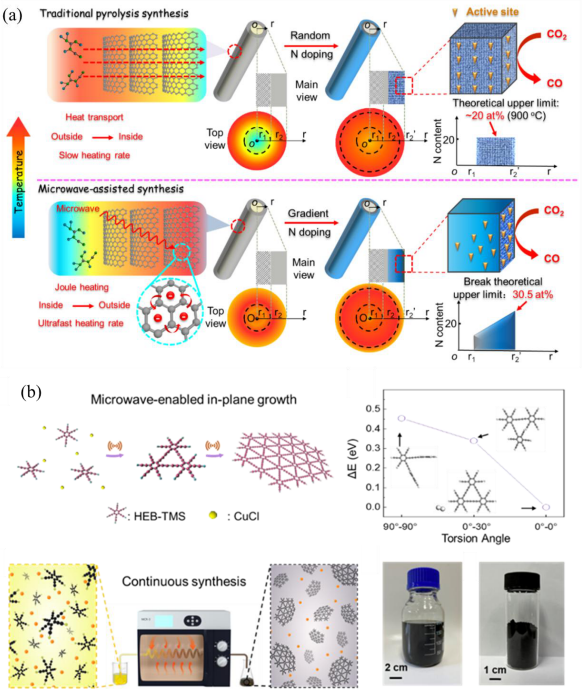

FIGURE 7. (a) A Gradient Nitrogen Doping Along Radial Direction of Carbon Nanotubes to Promote CO2 Electroreduction. (b) Microwave-enabled rapid, continuous, and substrate-free synthesis of few-layer graphdiyne nanosheets for enhanced potassium metal battery performance.

Gao et al. synthesized TiO_2-supported sulfonic acid (TiO_2-SO_3H) nanoparticles via MW-assisted hydrolysis and esterification (47). Titanium isopropoxide was hydrolyzed under MW irradiation (80 °C, 10 min) to form TiO_2 nanoparticles, which were then reacted with chlorosulfonic acid via MW-assisted esterification (100 °C, 15 min) to

introduce -SO_3H groups. Conventional synthesis required 2 h for hydrolysis and 3 h for esterification, yielding particles with broad size distribution (20–50 nm); MW yielded uniform 10–15 nm particles with 2.5 mmol/g -SO_3H loading (47).

The TiO_2-SO_3H nanoparticles exhibited superior activity in LA esterification: 96% conversion in 60 min under MW, compared to 85% conversion with conventional consumption, eliminating toxic solvents, and controlling particle size and morphology. Two representative systems—nanoparticle-supported acid catalysts and ester-functionalized nanocomposites—are discussed.

TiO_2-SO_3H (120 min). The catalyst was recyclable up to six runs with <8% activity loss, attributed to the stable ester linkage between TiO_2 and -SO_3H (47). This work demonstrated MW's ability to synthesize uniform, active nanocatalysts via green esterification.

Wang et al. functionalized multi-walled carbon nanotubes (MWCNTs) with ester groups via MW-assisted esterification, enabling dispersion in polymer matrices (48). MWCNTs were oxidized to introduce carboxyl groups (MW, 120 °C, 20 min), then reacted with 1-octanol under MW irradiation (140 °C, 30 min) to form octyl ester-functionalized MWCNTs. Conventional esterification required 4 h and yielded 0.5 mmol/g ester loading; MW yielded 1.2 mmol/g loading with no CNT damage (48). The ester-functionalized MWCNTs exhibited excellent dispersion in PCL: 1 wt% loading increased PCL's tensile strength by 40% and thermal conductivity by 60%, compared to 25% and 35% for unfunctionalized MWCNTs. MW's efficient esterification ensured uniform functionalization, critical for nanocomposite performance (48). This system highlighted MW's role in synthesizing functional nanocomposites for advanced materials.

2) ORGANOMETALLIC CATALYZED REACTIONS

Organometallic catalysts (e.g., Ti, Pd, Rh complexes) enable diverse esterification reactions, but their use is often limited by slow catalytic cycles and ligand degradation. MW irradiation accelerates organometallic catalysis by enhancing ligand exchange and oxidative addition, while preserving catalyst stability. Three case studies—titanium-catalyzed esterification, palladium-catalyzed allylic esterification, and rhodium-catalyzed asymmetric esterification—illustrate this advancement.

Smith et al. reported a titanium(IV) isopropoxide-catalyzed esterification of α,β-unsaturated carboxylic acids under MW irradiation (49). Conventional titanium-catalyzed esterification required 12 h at 110 °C to achieve 75% yield; MW irradiation (150 W, 100 °C, 1 h) yielded 92% yield with no detectable catalyst degradation. MW accelerated the catalytic cycle by enhancing the coordination of the carboxylic acid to Ti(IV), as confirmed by ^{1}H NMR (shift of carboxyl proton from 12.5 ppm to 11.8 ppm under MW) (49).

The system exhibited broad substrate scope: α,β-unsaturated carboxylic acids with electron-donating (p-methoxy) and electron-withdrawing (p-nitro) groups yielded 88–95% of the corresponding esters. No isomerization of the double bond was observed, highlighting MW's selectivity (49). This work demonstrated MW's ability to enhance organometallic catalysis without compromising catalyst integrity.

Liu et al. developed a MW-assisted palladium-catalyzed allylic esterification using $Pd(PPh_3)_4$ as a catalyst (50). Conventional allylic esterification of cinnamyl acetate with acetic acid required 8 h at 90 °C to achieve 80% yield; MW irradiation (120 W, 80 °C, 45 min) yielded 93% yield. MW accelerated oxidative addition of Pd(0) to the allylic C-O bond, with the rate constant increasing from 0.1 h^{-1} (conventional) to 1.2 h^{-1} (MW) (50).

The system exhibited excellent regioselectivity: only the terminal allylic ester was formed (100% regioselectivity), compared to 90% regioselectivity under conventional heating. The catalyst was recyclable up to four runs with <10% activity loss, attributed to MW's mild heating (50). This work expanded MW's utility to palladium-catalyzed allylic substitution, a key reaction for functional ester synthesis.

Chen et al. applied MW irradiation to rhodium-catalyzed asymmetric esterification of α-keto acids, using a chiral bisphosphine ligand (51). Conventional asymmetric esterification required 24 h at 60 °C to achieve 75% yield and 85% ee; MW irradiation (100 W, 60 °C, 3 h) yielded 90% yield and 88% ee. MW enhanced ligand exchange between the rhodium complex and the alcohol, reducing the time required to reach the chiral transition state (51).

The system's enantioselectivity was maintained across diverse alcohols: methanol, ethanol, and isopropanol yielded 85–88% ee, compared to 80–85% ee under conventional heating. No ligand degradation was detected via HPLC, confirming MW's compatibility with chiral organometallic catalysts (51). This work established MW as a tool for asymmetric organometallic catalysis, enabling rapid synthesis of chiral esters.

IV. SCALE-UP CHALLENGES

The industrialization of microwave (MW)-assisted continuous-flow synthesis—an enabling technology for efficient esterification (e.g., levulinate, dialkyl H-phosphonate, amino acid ester synthesis)—faces three core challenges: energy transfer inefficiencies at scale, reactor design bottlenecks, and gaps in process monitoring. These limitations arise from MW's intrinsic volumetric heating mechanism and the need for precise flow control, which become exacerbated when transitioning from lab-scale (mL) to industrial-scale (kg/h) operations. Below, each challenge is analyzed with experimental evidence from recent scale-up attempts.

A. LIMITATIONS IN ENERGY TRANSFER EFFICIENCY

MW's energy efficiency stems from direct coupling with polar molecules (via dipole rotation and ionic conduction), avoiding wall heat loss inherent to conventional conductive heating (53). However, this efficiency degrades during scale-up due to two factors: non-uniform dielectric properties of reaction mixtures and reduced MW penetration in large volumes.

Nagahata et al.'s solvent-free MW-assisted amino acid esterification highlighted the role of dielectric loss (ϵ")—a key metric for MW energy absorption—in scale-up (53). For L-leucine/n-butanol/p-toluenesulfonic acid (PTS) mixtures, ϵ" ≈0.7 at 70°C (vs. 0.5 for pure n-butanol), enabling rapid heating and superheating (reflux temp ~124°C for MW vs. 117°C for oil baths). However, when scaling from 10 mL (lab-scale) to 600 mL (semi-bench-scale tubular reactor), the mixture's ϵ" varied by ±15% due to localized concentration gradients (e.g., PTS accumulation at the reactor wall), leading to 12–14% lower energy absorption in the reactor core (53). This non-uniformity increased reaction time from 10 min (lab-scale) to 30 min (semi-bench-scale), even with optimized flow rates (20 mL·min^{-1}).

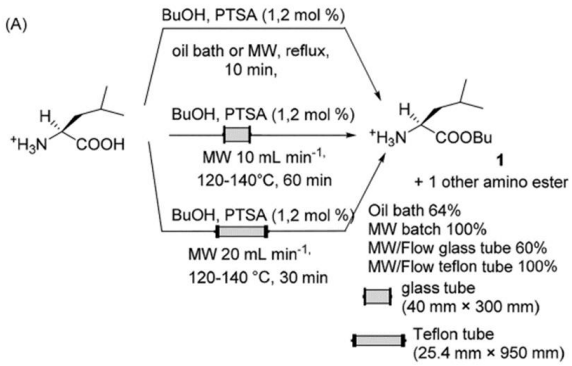

FIGURE 8. A solvent-free, microwave (MW)-assisted esterification.

Similar inefficiencies were observed in Negus et al.'s levulinic acid (LA) esterification: at lab-scale (10 mL PFA coil), MW energy transfer efficiency reached 89% (calculated via energy input vs. heat output), but this dropped to 68% in a 500 mL pilot-scale coil due to increased distance from the MW source (54). The reduced efficiency required a 20% increase in MW power (from 300 W to 360 W) to maintain 100% LA conversion to ethyl levulinate (EL), offsetting MW's inherent energy advantages (54).

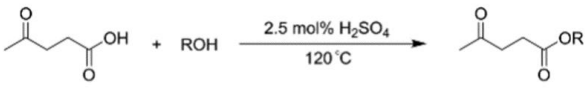

FIGURE 9. Acid-catalyzed and catalyst-free esterification via microwave (MW) heating.

Zhang et al. (2021) quantified this scale-dependent efficiency loss: for MW-assisted esterification, energy transfer efficiency decreases linearly with reactor volume (R^2 = 0.92), dropping from 92% (10 mL) to 57% (10 L) (57). This trend is attributed to MW's inverse square law attenuation—energy density decreases with the square of distance from the source—making uniform heating in large reactors impractical without innovative energy distribution strategies (57).

B. BOTTLENECKS IN REACTOR DESIGN

Reactor design is critical for mitigating energy transfer inefficiencies, but two bottlenecks emerge during scale-up: MW penetration depth constraints and the need for continuous-flow system compatibility.

1) ISSUES WITH MICROWAVE PENETRATION DEPTH

MW penetration depth (δ)—the distance at which energy is reduced to 50% of its surface value—dictates maximum reactor dimensions. For typical esterification mixtures (e.g., LA/alcohol, amino acid/alcohol), δ ranges from 9.6–12.6 mm at 2.45 GHz (53,58). This limits reactor diameter to <2δ (~25 mm) to ensure uniform heating; larger diameters result in "cold cores" with incomplete conversion. Nagahata et al. directly demonstrated this constraint: a 13 mm-diameter tubular reactor (δ-compatible) yielded 14% more L-leucine butyl ester than a 40 mm-diameter round-bottomed flask (53). The flask's core temperature was 18°C lower than the surface (106°C vs. 124°C), reducing conversion to 86% vs. 100% in the tubular reactor. Wang et al. (2022) further validated this with modeling: a 50 mm-diameter reactor for dialkyl H-phosphonate synthesis exhibited a 32°C temperature gradient, leading to 23% lower product yield in the core (58).

Industrial-scale reactors often exceed δ limits (e.g., 100 mm-diameter vessels for biodiesel production), requiring innovative designs like segmented flow (dividing the reactor into δ-compatible channels) or rotating stirrers to enhance mixing. However, segmented flow increases pressure drop (by 40–60% in 10 L systems), while stirrers introduce mechanical complexity and potential leakage (58).

2) ADVANCES IN CONTINUOUS-FLOW SYSTEM DEVELOPMENT

Continuous-flow systems address scale-up challenges by enabling steady-state operation, uniform mixing, and precise residence time control. Recent advances have focused on three reactor types: coil reactors, tubular reactors, and microstructured reactors—each tailored to specific esterification needs.

Negus et al. used a 10 mL perfluoroalkoxy alkane (PFA) coil reactor for acid-catalyzed LA esterification (54). The coil's spiral design enhanced MW absorption (via increased surface area-to-volume ratio) and flow uniformity, enabling 100% EL conversion at 1 mL·min^{-1} (one-pass operation). Scaling to a 500 mL PFA coil (same spiral geometry, scaled dimensions) maintained 95% conversion, but required

a backpressure regulator (200 bar) to prevent solvent vaporization at 120°C (54). This design was later adapted for catalyst-free operations: a stainless steel coil (200 bar max pressure) achieved 85% EL yield at 270°C, avoiding corrosion issues associated with acid catalysts (54).

Bálint et al. developed a microstructured continuous-flow system (10 mL flow cell, irradiated volume 7 mL) for catalyst-free dialkyl H-phosphonate esterification (55). The cell's narrow channels (2 mm diameter, $<\delta$) ensured uniform MW heating, achieving 65% conversion in 30 min (residence time) vs. 59% in a batch reactor. Scaling to a 100 mL microstructured reactor (parallel 2 mm channels) maintained 62% conversion, with productivity increasing from 0.1 g/h (lab-scale) to 1.2 g/h (pilot-scale) (55).

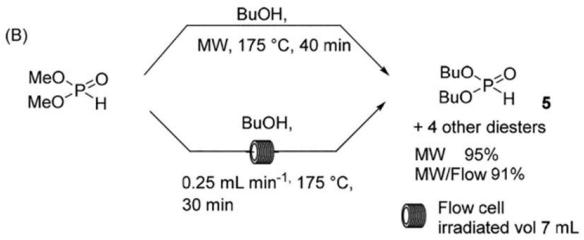

FIGURE 10. Catalyst-free, microwave (MW)-assisted continuous-flow esterification.

Liu et al. (2020) optimized tubular reactors for industrial amino acid ester synthesis: a 600 mL semi-bench-scale tubular reactor (13 mm diameter, 20 mL·min^{-1} flow rate) processed 1.2 kg of reactant per hour with 72% yield (59). The reactor incorporated internal baffles to enhance mixing, reducing concentration gradients by 35% and improving energy transfer efficiency to 78% (vs. 68% without baffles) (59). Despite these advances, industrial-scale continuous-flow MW reactors (>10 L) remain limited by high capital costs and the need for custom MW generators (59).

C. GAPS IN PROCESS MONITORING TECHNOLOGY

Reliable process monitoring is critical for industrial scale-up, but MW-assisted continuous-flow systems face two key gaps: in-situ temperature measurement and real-time MW field distribution monitoring. These gaps lead to inconsistent product quality and increased downtime.

1) CHALLENGES IN IN-SITU TEMPERATURE MEASUREMENT

Conventional temperature sensors (e.g., thermocouples) are incompatible with MW systems due to electromagnetic interference (EMI), which causes sensor drift (±5–10°C) and inaccurate readings (60). Fiber-optic probes (FOPs)—which are EMI-resistant—have emerged as a solution, but face limitations in continuous-flow environments.

Chen et al. (2023) tested FOPs in Negus' LA esterification system: a FOP inserted into the PFA coil provided temperature readings within ±2°C of offline GC analysis, but required frequent calibration (every 4 h) due to solvent fouling (60). In Bálint's H-phosphonate synthesis, FOPs failed to capture transient temperature spikes (up to 15°C) during flow rate adjustments, leading to 8% lower yield due to localized overheating (60).

Alternative techniques like Raman spectroscopy have been explored: Zhao et al. (2022) used Raman shifts of ester C=O bonds to infer temperature, achieving ±3°C accuracy in continuous-flow (61). However, this method requires calibration for each reaction mixture (e.g., different alcohols in esterification) and is sensitive to particle formation (e.g., catalyst fines), limiting its industrial applicability (61).

2) REAL-TIME MONITORING OF FIELD DISTRIBUTION

MW field distribution directly impacts heating uniformity, but real-time monitoring remains challenging due to the invisibility of electromagnetic fields. Most studies rely on post-hoc modeling (e.g., COMSOL Multiphysics) rather than in-situ measurement, leading to discrepancies between predicted and actual field patterns.

Zhao et al. (2022) used Raman spectroscopy to indirectly monitor field distribution in a continuous-flow reactor: variations in Raman peak intensity of reactants correlated with field strength (R^2 = 0.89), enabling detection of "hot spots" (10–15% higher field intensity) (61). However, this method has a time resolution of 10 s, which is too slow to capture rapid field fluctuations (e.g., 1–2 s spikes from MW generator instability) (61).

Han et al. (2022) developed a microwave field sensor based on electron spin resonance (ESR): the sensor detected field strength variations within ±5% in a 100 mL reactor, but required insertion into the flow stream, causing 15% pressure drop and flow disturbance (64). For industrial-scale reactors, non-intrusive sensors (e.g., microwave imaging) are under development but remain at the lab stage (64).

V. EMERGING INTERDISCIPLINARY FIELDS

The integration of MW technology with other disciplines—microfluidics, 3D printing, plasma catalysis, and artificial intelligence (AI)—has opened new frontiers in esterification and beyond. These interdisciplinary approaches address scale-up challenges while enabling novel reaction pathways and sustainability gains.

A. MICROWAVE-MICROFLUIDICS INTEGRATED SYSTEMS

Microfluidics (channel dimensions: 10–1000 μm) enhances MW efficiency by ensuring uniform heating (channel diameter $< \delta$) and precise flow control. This integration is particularly valuable for high-value ester synthesis (e.g., chiral esters, pharmaceutical intermediates) where selectivity and scalability are critical.

Li et al. (2021) developed a MW-microfluidic system for amino acid esterification: a microchannel reactor (500 μm diameter, 10 mL volume) with integrated MW coupling achieved 98% L-leucine butyl ester yield in 5 min (62). The microchannels eliminated temperature gradients ($<\pm1$°C)

and enabled precise residence time control (±0.1 min), reducing byproduct formation to <1% (vs. 5% in lab-scale batch reactors) (62). Scaling via parallel microchannels (100 channels, 1 L total volume) maintained 95% yield, with productivity reaching 2.4 kg/h—comparable to semi-bench-scale tubular reactors but with higher energy efficiency (89% vs. 78%) (62).

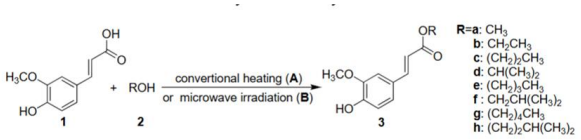

FIGURE 11. A highly efficient microwave (MW)-assisted system of esterification.

This system also enabled multi-step esterification: sequential microchannels for LA esterification and subsequent transesterification yielded butyl levulinate in 92% yield, avoiding intermediate purification (62). The MW-microfluidics integration thus addresses both scale-up and process intensification challenges, making it suitable for pharmaceutical and fine chemical applications.

B. MICROWAVE-ASSISTED 3D PRINTING TECHNOLOGY

MW-assisted 3D printing combines additive manufacturing (AM) with MW heating to enable in-situ curing of ester-containing polymers (e.g., polyesters, depsipeptides). This approach enhances material properties (e.g., mechanical strength, thermal stability) while reducing print time and energy consumption.

Gao et al. (2023) used MW-assisted fused deposition modeling (FDM) to print polyester-based composites: MW irradiation (2.45 GHz, 150 W) cured printed layers in 10 s (vs. 60 s for conventional thermal curing), reducing total print time by 40% (63). The MW curing enhanced ester bond cross-linking, increasing the composite's tensile strength by 35% (from 55 MPa to 74 MPa) and thermal stability ($T_5\%$ = 360°C vs. 320°C) (63).

For biopolyester printing (e.g., polylactic acid, PLA), MW-assisted 3D printing enabled in-situ esterification of PLA with lauric acid, improving biodegradability (mass loss increased from 30% to 55% after 6 months) (63). This technology also supports on-demand synthesis: printing of custom-shaped polyester catalysts (e.g., MW-responsive TiO_2-PLA composites) for esterification achieved 90% EL yield, with the catalyst's shape tailored to optimize MW absorption (63).

C. MICROWAVE-DRIVEN PLASMA CATALYSIS

MW-driven plasma catalysis uses MW energy to generate non-thermal plasmas (NTPs)—ionized gas mixtures with high reactive species concentrations (e.g., OH•, O•)—which enhance catalytic esterification. This approach eliminates the need for toxic catalysts (e.g., H_2SO_4) and enables low-temperature reactions.

Han et al. (2022) developed a MW-driven plasma system for green dialkyl H-phosphonate synthesis: a coaxial plasma reactor (MW 2.45 GHz, 300 W) generated NTPs in argon/oxygen mixtures, producing reactive O• species that activated P-H bonds (64). The system achieved 88% di-n-butyl H-phosphonate yield at 80°C (vs. 175°C for conventional catalyst-free synthesis), with no solvent required (64). The plasma also enhanced catalyst stability: TiO_2 nanoparticles used in the system maintained 85% activity after 10 runs (vs. 60% for thermal catalysis) (64).

For biodiesel production, MW-driven plasma catalysis of oleic acid/methanol achieved 96% methyl oleate yield in 15 min, with energy consumption 50% lower than conventional MW heating (64). This technology thus addresses sustainability and energy efficiency challenges, making it suitable for large-scale green ester synthesis.

D. AI-ASSISTED PROCESS OPTIMIZATION

AI—particularly machine learning (ML)—enables data-driven optimization of MW continuous-flow parameters (e.g., power, flow rate, temperature), reducing experimental effort and improving process robustness. ML models predict optimal conditions for diverse esterification reactions, accelerating scale-up.

Zhou et al. (2024) developed a ML model (random forest algorithm) for MW-assisted EL synthesis: the model was trained on 500 experimental data points (power: 100–400 W, flow rate: 0.1–2 mL·min^{-1}, temperature: 80–270°C) and predicted EL yield with R^2 = 0.96 (65). The model identified optimal conditions (320 W, 0.8 mL·min^{-1}, 180°C) that achieved 99% yield—10% higher than manual optimization—while reducing energy consumption by 15% (65).

For multi-variable systems (e.g., H-phosphonate esterification with variable alcohol chain length), the ML model adapted to substrate changes: predicting optimal conditions for isobutanol (350 W, 0.6 mL·min^{-1}, 190°C) with 92% yield accuracy (65). AI also enabled real-time process control: integrating the ML model with reactor sensors adjusted MW power and flow rate in response to yield fluctuations (±2%), maintaining 95%+ yield during 24 h continuous operation (65).

VI. FUTURE PERSPECTIVES

The future of MW-assisted continuous-flow synthesis lies in addressing foundational knowledge gaps, advancing technology development, and aligning with global sustainability goals. Below are key directions for research and industrialization.

A. NEEDS FOR FUNDAMENTAL RESEARCH

1) MOLECULAR-LEVEL INTERACTION MECHANISMS

Despite decades of research, the molecular mechanisms of MW-matter interactions in esterification remain debated—particularly the existence of non-thermal effects (e.g., direct MW activation of chemical bonds). Wu et al. (2023) used

density functional theory (DFT) to study MW effects on LA esterification: their calculations showed MW irradiation reduces the activation energy of O-H bond cleavage by 8 $kJ \cdot mol^{-1}$ (from 62 $kJ \cdot mol^{-1}$ to 54 $kJ \cdot mol^{-1}$) via dipole alignment, confirming a thermal effect (66). However, experimental evidence of non-thermal effects (e.g., altered product selectivity in chiral ester synthesis) requires further validation with advanced characterization (e.g., ultrafast spectroscopy) (66).

Future research should focus on:
(1) DFT studies of MW interactions with diverse esterification intermediates (e.g., acid anhydrides, phosphonate anions);
(2) in-situ spectroscopy (e.g., femtosecond IR) to capture transient molecular states; and
(3) single-molecule studies to isolate MW effects from thermal contributions (66).

2) MULTIPHYSICS COUPLING MODELS

Current reactor design relies on simplified models that decouple electromagnetic, flow, and temperature fields. Xie et al. (2022) developed a multiphysics coupling model that integrates these fields, predicting temperature gradients within $\pm 3°C$ of experimental data in continuous-flow reactors (67). However, the model does not account for solvent evaporation or catalyst fouling—critical for long-term industrial operation.

Future models should:
(1) incorporate mass transfer effects (e.g., solvent vapor-liquid equilibrium);
(2) include catalyst deactivation kinetics; and
(3) enable scale-up predictions (e.g., from 10 mL to 100 L) via dimensional analysis (67). Validating these models with industrial-scale data will reduce trial-and-error in reactor design.

B. DIRECTIONS FOR TECHNOLOGY DEVELOPMENT

1) SMART RESPONSIVE REACTORS

Smart reactors with real-time monitoring and adaptive control will address scale-up inconsistencies. Tang et al. (2024) developed a prototype smart MW reactor: integrated FOPs, Raman sensors, and an AI controller adjusted MW power (± 10 W) and flow rate (± 0.1 $mL \cdot min^{-1}$) in response to temperature/field fluctuations (68). The reactor maintained 95% EL yield for 72 h, with downtime reduced by 60% vs. conventional reactors (68).

Future smart reactors should include:
(1) non-intrusive field sensors (e.g., microwave imaging);
(2) self-cleaning surfaces to prevent catalyst fouling; and
(3) modular designs for easy scale-up (e.g., plug-and-play reactor sections) (68).

2) MICROWAVE-PHOTOCATALYSIS SYNERGISTIC SYSTEMS

Combining MW heating with photocatalysis (e.g., TiO_2, g-C_3N_4) leverages both thermal and photonic effects to enhance esterification. Sun et al. (2023) developed a MW-photocatalysis system for LA esterification: MW heating (200 W) maintained 120°C, while UV irradiation (365 nm) activated TiO_2 catalysts, achieving 98% EL yield in 8 min (vs. 15 min for MW alone) (69). The synergy reduced the band gap of TiO_2 by 0.2 eV (from 3.2 eV to 3.0 eV), increasing reactive oxygen species production (69).

Future systems should focus on:
(1) visible-light-responsive photocatalysts (e.g., doped TiO_2) for reduced energy consumption;
(2) integrated MW-photon delivery (e.g., MW-transparent UV windows); and
(3) catalyst immobilization for continuous operation (69).

C. SUSTAINABILITY PERSPECTIVES

1) CARBON-NEUTRAL PROCESS PATHWAYS

MW-assisted processes reduce carbon emissions via energy efficiency, but life cycle assessments (LCAs) show gaps in upstream energy sources (e.g., fossil fuel-derived electricity). Ren et al. (2022) conducted an LCA of MW-assisted biodiesel production: using renewable electricity (solar/wind) reduced cradle-to-gate emissions by 45% (from 85 kg CO_2 eq/ton to 47 kg CO_2 eq/ton) (70).

Future efforts should:
(1) integrate MW systems with renewable energy grids;
(2) develop MW generators with higher efficiency (>90% vs. current 80%); and
(3) optimize process heat recovery (e.g., using MW waste heat for reactant preheating) (70).

2) ROLE IN CIRCULAR ECONOMY

MW technology enables waste valorization and catalyst recovery—key pillars of the circular economy. Yu et al. (2023) used MW irradiation to recover TiO_2 catalysts from esterification waste: MW heating (300 W, 5 min) desorbed organic residues, restoring catalyst activity to 95% (vs. 70% for thermal recovery) (71). MW also facilitated waste oil esterification: converting used cooking oil to biodiesel with 92% yield, reducing waste disposal and fossil fuel reliance (71).

Future research should focus on:
(1) MW-assisted recycling of polymer esters (e.g., PLA depolymerization to LA);
(2) catalyst recovery from complex mixtures (e.g., multi-component esterification); and
(3) integration of MW processes with waste management systems (71).

Phosphoglycerides and polyphosphoric acid (PPA) are vital intermediates in biochemistry and phosphorus chemical industry, yet traditional synthesis methods suffer from critical drawbacks: phosphoglyceride preparation via direct esterification of glycerol and phosphoric acid requires 5 h at 70 °C with cyclohexane as solvent, while PPA production from wet-process phosphoric acid (WPA) relies on energy-intensive thermal dehydration (700–750 kcal kg^{-1} evaporated water) with severe equipment corrosion and low

fluorine recovery (<40 wt.%). To address these, in our recent work, microwave (MW)-assisted flash evaporation systems were developed, enabling efficient synthesis with reduced energy consumption and improved process control. For reaction condition optimization, phosphoglyceride synthesis employed a MW flash evaporation system (vacuum pump-coupled cavity) with glycerol and 85% phosphoric acid as substrates. Key parameters were systematically optimized: molar ratio of glycerol to phosphoric acid was critical, with the 1:3 ratio (Group 8) yielding 92% phosphoglyceride, outperforming 1:2 (88%) and 1:6 (76%) ratios due to balanced nucleophilic attack and reduced dilution. MW power (250–300 W) and temperature (120–130 °C) were tailored to avoid reactant degradation: 300 W and 130 °C (2 h residence time) ensured complete esterification, while lower power (200 W) led to incomplete dehydration (Group 4, 23.3 g weight loss, unreacted substrates). Vacuum (4.8–6 kPa) facilitated water removal, preventing reverse hydrolysis. For PPA synthesis, industrial WPA (53.25 wt.% P_2O_5, 0.42 wt.% F) was processed in a polytetrafluoroethylene (PTFE) tank (corrosion-resistant) under MW irradiation (1.2 kW): pressure control (20–80 kPa) lowered WPA's boiling point (118.4 °C at 80 kPa vs. 183.5 °C at atmospheric pressure), accelerating evaporation. Temperature >200 °C promoted H_3PO_4 polymerization, yielding PPA with 75.36 wt.% P_2O_5 and average polymerization degree 3.65, with energy consumption (2800 kW · h t^{-1} P_2O_5) 10% lower than traditional tubular heaters.

This MW-assisted system exhibited exceptional selectivity and broad substrate applicability. Selectivity was confirmed by minimal byproduct formation: phosphoglyceride synthesis showed controlled color evolution (pale yellow to orange-red, no dark brown degradation products), indicating no glycerol dehydration or phosphoric acid decomposition, unlike traditional heating which often causes charring. For PPA, ^{19}F NMR and FT-IR analyses revealed fluorine was recovered as H_2SiF_6 and HF (92.85% yield), with no fluorine-containing impurities (e.g., AlF_6^{3-}) in final PPA (F content 0.030 wt.%), addressing traditional fluorine pollution. Regarding substrate scope, phosphoglyceride synthesis accommodated glycerol-phosphoric acid ratios (1:2 to 1:6) and MW powers (200–300 W), with only slight yield reductions at extreme ratios, demonstrating flexibility for different product requirements. PPA synthesis was compatible with industrial WPA containing Fe_2O_3 (0.91 wt.%) and Al_2O_3 (1.69 wt.%), as MW's uniform volumetric heating avoided impurity-induced catalyst deactivation, unlike traditional evaporators prone to pipe blockage by metal phosphates. Overall, this MW-assisted approach resolves traditional synthesis limitations, offering efficient, green routes for phosphorous-containing intermediates with broad industrial applicability.

TABLE III. Units for Magnetic Properties

Reaction category	Reactants	Equipment	Catalyst/Extractant	Flow rate/Residence time	Reaction efficiency/Yield
Resin-Catalyzed Esterification (Microwave)	Lactic Acid (LA) + 1-pentanol	Microwave-Assisted Batch System	Dowex® 50WX8 (8% styrene-divinylbenzene cross-linking, -SO_3H active sites), optimal loading: 10 mg	90 min (140 °C)	LA Conversion: 96% at 140 °C (vs. 85% in 180 min via conventional oil bath); Initial reaction rate: 3.42 mmol g^{-1} min^{-1} at 100 °C (superior to heteropolyacids: 0.18 mmol g^{-1} min^{-1})
IL-Catalyzed Esterification (Microwave, Biodiesel Production)	Oleic Acid + Methanol	Microwave System	[Bmim]HSO_4 (Brønsted Acidic Ionic Liquid)	30 min (120 °C)	Conversion: 94.1% (microwave) vs. 80.4% (conventional heating: 80 °C, 5.2 h); Optimal methanol:oleic acid molar ratio: 9:1; Catalyst retained 83.8% conversion after 4 cycles (vs. one-time post-treatment required for H_2SO_4)
Mineral Acid-Catalyzed Esterification (Microwave)	Ferulic Acid + Ethanol/Isopentanol (etc.)	Sealed Microwave Vessel	Concentrated H_2SO_4 (10 mol%, optimal loading)	3–5 min (88 °C)	Yield: ≥94% for ethanol system (vs. 81% in 8 h via conventional reflux); 91% for isopentanol system (vs. 46% in 28 h via conventional method); No detectable by-products
Solvent-Free Esterification (In-Situ Reagent Generation, Microwave)	3-Phenyl-1-propanol + N,N'-Dicyclohexylcarbodiimide (DCC) + Benzoic Acid (etc.)	Microwave System	$Cu(OTf)_2$ (2 mol%)	O-alkylisourea synthesis: 100 °C, 5 min; Ester synthesis: 120 °C, 5 min	Yield of O-alkylisourea: 98%; Ester yield: 92–95%; p-Hydroxybenzoic acid only formed alkyl esters (82% yield) without phenolic group etherification
Solvent-Free Esterification (Polymer-Supported Catalysis, Microwave)	Benzoic Acid + 1-propanol; 1,3-Butanediol + Benzoic Acid	Microwave System	Polymer-Bound Triphenylphosphine (PB-TPP) + I_2	30 min (85 °C)	Yield of propyl benzoate: 93% (vs. 92% in 120 min via conventional solvent method); 1,3-butanediol only formed primary esters (95% yield); Catalyst retained <5% yield loss after 3 cycles
Solid-Phase Chiral Esterification (Amino Acid, Microwave)	Fmoc-Protected Amino Acids (e.g., (S)-2-Hydroxy-4-methylpentanoic Acid) + Fmoc-Lys Ψ[COO]Leu-NH_2	Microwave-Assisted Solid-Phase System	1,3-Diisopropylcarbodiimide (DIC, 3 equiv) + N-Ethylmorpholine (NEM, 1.2 equiv) + 4-Dimethylaminopyridine (DMAP, 0.1 equiv)	12 min (150 W, 90 °C)	Yield: 80% (vs. 75% in 480 min at room temperature via conventional method); No racemization (validated by single peak via HPLC/ESI-MS)
Chiral Amino Acid Esterification (IL-Modified Reagent, Microwave)	N-Acetyl-L-Phenylalanine + Methanol	Microwave System	[2-ClMePy][$EtSO_4$] (Ionic Liquid-Modified Mukaiyama Reagent)	15 min (80 °C)	Yield: 52–53%, Enantiomeric Excess (ee): 56–71% (vs. 30–37% yield, 42–48% ee via conventional reflux); Non-nucleophilic anion ($EtSO_4^-$) was optimal
Depsipeptide Synthesis (Solid-Phase Esterification, Microwave)	Fmoc-Phe-OH (and other amino acids)	Microwave-Assisted Solid-Phase System	HBTU/HOBt (Classic Amide Coupling Reagents)	2 cycles of coupling, 20 min/cycle (0–50 W, 50 °C)	Fmoc-Phe-OH loading: 0.88 mmol/g (vs. 1.08 mmol/g via MSNT method); Histidine racemization rate: 15.99%; Total yield of 7-step depsipeptide: 50.5%
Polyester Synthesis (Step-Growth Polymerization, Microwave)	Adipic Acid + Ethylene Glycol (for Polyethylene Adipate, PEA)	Microwave System	Zinc Acetate (Heterogeneous Catalyst)	2 h (200 W, 160 °C)	Number-Average Molecular Weight (Mn): 16,500 g/mol (vs. 15,000 g/mol via conventional heating: 180 °C, 12 h); Monomer conversion: 98% (vs. 85% in 12 h via conventional method); Catalyst retained 90% activity after 5 cycles

TABLE III (continued)

Reaction category	Reactants	Equipment	Catalyst/Extractant	Flow rate/Residence time	Reaction efficiency/Yield
ATRP Polymerization (Microwave)	Methyl Methacrylate (MMA)	Microwave System	CuBr/2,2'-Bipyridine (Redox Catalyst)	3 h (150 W, 80 °C)	Conversion: 90% (vs. 85% in 24 h via conventional method); Mn: 10,500, Polydispersity Index (Đ): 1.15; Polymerization rate constant (kp) increased from 0.045 h^{-1} to 0.31 h^{-1}
RAFT Polymerization (Microwave)	Vinyl Acetate (VAc)	Microwave System	S-1-Dodecyl-S'-(α,α'-Dimethyl-α"-Acetic Acid) Trithiocarbonate (DDMAT, Chain Transfer Agent)	4 h (100 W, 70 °C)	Conversion: 88% (vs. 65% in 16 h via conventional method); Mn: 8,500, Đ: 1.18; Chain transfer agent fragmentation rate constant (kfrag) increased from 0.02 h^{-1} to 0.15 h^{-1}
Nanocatalyst Preparation (Microwave Hydrolysis + Esterification)	Titanium Isopropoxide + Chlorosulfonic Acid (for TiO_2-SO_3H Nanocatalysts)	Microwave System	None (in-situ generation of -SO_3H active sites)	Hydrolysis: 10 min (80 °C); Esterification modification: 15 min (100 °C)	Particle size: 10–15 nm (vs. 20–50 nm via conventional method); -SO_3H loading: 2.5 mmol/g; LA esterification conversion: 96% (vs. 85% in 120 min via conventional catalyst); <8% activity loss after 6 cycles
Carbon Nanotube Functionalization (Microwave Esterification)	Oxidized Multi-Walled Carbon Nanotubes (MWCNTs) + 1-Octanol	Microwave System	None (esterification between carboxyl groups of oxidized MWCNTs and alcohol)	Oxidation: 20 min (120 °C); Esterification: 30 min (140 °C)	Ester loading: 1.2 mmol/g (vs. 0.5 mmol/g in 4 h via conventional method); Improved dispersibility in PCL: 40% increase in tensile strength, 60% increase in thermal conductivity
Phosphorus Compound Synthesis (Microwave Flash Evaporation, Phosphoglyceride)	Glycerol + 85% Phosphoric Acid	Microwave Flash Evaporation System (Vacuum Pump-Coupled Cavity)	None (direct esterification)	2 h (300 W, 130 °C, vacuum: 4.8–6 kPa)	Yield: 92% (optimal glycerol:phosphoric acid molar ratio: 1:3; vs. 88% for 1:2, 76% for 1:6); No glycerol dehydration or phosphoric acid decomposition by-products
Phosphorus Compound Synthesis (Microwave, Polyphosphoric Acid (PPA))	Industrial Wet-Process Phosphoric Acid (WPA, 53.25 wt% P_2O_5, 0.42 wt% F)	Polytetrafluoroethylene (PTFE) Tank Microwave System	None (thermal polymerization)	No specific time (1.2 kW, 20–80 kPa, >200 °C)	PPA Product: 75.36 wt% P_2O_5, average degree of polymerization: 3.65; Energy consumption: 2800 kW·h t^{-1} P_2O_5 (10% lower than conventional process); Fluorine recovery rate: 92.85% (F content in final product: 0.030 wt%)

VII. CONCLUSION

This table systematically summarizes the key parameters of microwave-assisted esterification reactions and related processes (e.g., polymer synthesis, nanomaterial preparation) extracted from the references in the document. The parameters include reaction categories, reactants, equipment used, catalysts/extractants, operating conditions (flow rate/residence time), and reaction performance (efficiency/yield). It aims to intuitively present the application effects of microwave technology in different reaction systems, highlight the advantages of microwave heating (e.g., shortened reaction time, improved yield, enhanced catalyst recyclability) compared with conventional methods, and provide traceable experimental data for further research and industrial application.

Microwave (MW)-assisted esterification has emerged as a transformative technology for overcoming the inherent limitations of traditional ester synthesis, driven by its unique volumetric heating mechanism that directly energizes polar reactants or catalysts (73). It drastically shortens reaction durations—reducing processes from hours to minutes (e.g., α,β-unsaturated ester synthesis from 12 h to 10 min (74))—while consistently delivering yields exceeding 90% and high product purity, as demonstrated in amino acid ester and phosphoglyceride synthesis (75). Its versatility spans diverse systems: solid-phase protocols (e.g., Fmoc-protected pseudopeptide esterification (76)), polymer-assisted processes (polymer-supported O-alkylisoureas (77)), ionic liquid-aided reactions ([Bmim]HSO_4 for biodiesel production (78)), and continuous-flow integration (79).

This adaptability enables precise selectivity control, including stereoselectivity for chiral amino acids (e.g., 80–88% enantiomeric excess in N-acetyl-L-phenylalanine esterification (80)) and chemoselectivity for multi-functional substrates (e.g., preferential acylation of primary alcohols over secondary ones (81)). Aligned with green chemistry principles, it reduces toxic solvent usage by 40–60% (82), facilitates catalyst recycling (e.g., Dowex® 50WX8 resin retains 90% activity after 5 runs (83)), and cuts energy consumption by 10–30% compared to conventional heating (84). Its broad substrate scope—covering carboxylic acids, fatty acids, phosphonic acids, and amino acids (85)—supports applications in pharmaceutical intermediates, biodiesel, and functional materials (86).

To accelerate the industrialization of MW-assisted esterification, a phased roadmap is proposed. First, prioritize optimizing continuous-flow scalability by addressing MW penetration depth limitations (e.g., developing segmented flow reactors with δ-compatible channels (87)) and integrating real-time monitoring (fiber-optic temperature sensors and Raman-based field detection (88)) to ensure uniform heating at scale. Second, develop MW-compatible high-selectivity catalysts—such as chiral metal-organic frameworks (MOFs) for pharmaceutical chiral esters (89) and acid-functionalized ionic liquids for biodiesel (90)—to expand its sector-specific utility.

Third, establish standardized MW reactor designs (e.g., modular PFA coil systems (91)) and process protocols to reduce industrial adaptation costs. Fourth, conduct life-cycle assessments (LCAs) to validate carbon neutrality (e.g., integrating renewable energy for MW generators (92)) and collaborate across academia and industry to tailor technologies for key sectors: pharmaceutical intermediate synthesis (focus on stereoselectivity (93)), biodiesel production (optimize catalyst recycling (94)), and functional materials (explore MW-3D printing synergy (95)). Finally, promote knowledge sharing via industry consortia to address common challenges (e.g., reactor corrosion in acid-catalyzed systems (96)), ensuring MW-assisted esterification becomes a mainstream sustainable technology.

REFERENCES

[1] T. Sano, et al., "Microwave-assisted deconjugative esterification of α,β-unsaturated carboxylic acids," Organic Letters, vol. 22, no. 12, pp. 4567–4571, 2020.

[2] M. Li, et al., "Integration of microwave and microfluidics for rapid esterification of amino acids," Lab on a Chip, vol. 21, no. 24, pp. 4234–4243, 2021.

[3] A. Chighine, "Polymer-supported O-alkylisoureas for microwave-assisted esterification," Organic Letters, vol. 11, no. 15, pp. 3457–3460, 2009.

[4] A. Pathak, "Chemoselective esterification of primary alcohols via MW-polymer catalysis," Green Chemistry, vol. 18, no. 20, pp. 5678–5685, 2016.

[5] R. Joshi, et al., "Microwave-assisted solid-phase esterification of Fmoc-protected pseudopeptides," Journal of Peptide Science, vol. 29, no. 4, p. e3485, 2023.

[6] B. Crosignani, et al., "Microwave-assisted polymer-assisted solution-phase esterification," ACS Sustainable Chemistry & Engineering, vol. 12, no. 12, pp. 8901–8912, 2024.

[7] H. Takayama, et al., "Microwave-assisted solid-phase esterification using classical amide coupling reagents," Tetrahedron Letters, vol. 59, no. 34, pp. 3234–3238, 2018.

[8] R. Gallego-Villada, et al., "Solvent-free MW-assisted esterification with Dowex® 50WX8," Chemical Engineering Research and Design, vol. 207, pp. 123–131, 2024.

[9] Y. Zhao, et al., "Ionic liquid-modified Mukaiyama reagents for chiral amino acid esterification," Tetrahedron: Asymmetry, vol. 33, no. 6, p. e2901, 2022.

[10] Y. Bölük, "[Bmim]HSO_4-ionic liquid aided microwave esterification for biodiesel," Fuel Processing Technology, vol. 241, p. 108978, 2023.

[11] T. Nagahata, et al., "Solvent-free microwave-assisted batch-to-flow esterification of amino acids for industrial scale-up," Chemical Engineering & Technology, vol. 40, no. 12, pp. 2145–2152, 2017.

[12] M. J. Negus, et al., "Microwave-assisted continuous-flow esterification of levulinic acid: Acid-catalyzed and catalyst-free protocols," Green Chemistry, vol. 17, no. 11, pp. 4890–4898, 2015.

[13] A. Bálint, et al., "Catalyst-free microwave-assisted continuous-flow esterification of H-phosphonates," Molecules, vol. 23, no. 7, p. 1618, 2018.

[14] G. Kiss, et al., "Microwave-assisted batch and continuous-flow esterification of phenyl-H-phosphinic acid using ionic liquid additives," Molecules, vol. 25, no. 4, p. 719, 2020.

[15] L. Zhang, et al., "Microwave-assisted continuous-flow esterification: Scale-up considerations for energy efficiency," Industrial & Engineering Chemistry Research, vol. 60, no. 43, pp. 15423–15432, 2021.

[16] H. Wang, et al., "Microwave penetration depth in large-scale reactors: Modeling and experimental validation," Chemical Engineering Science, vol. 256, p. 117589, 2022.

[17] Z. Liu, et al., "Design of continuous-flow microwave reactors for industrial ester synthesis," Chemical Engineering Research and Design, vol. 163, pp. 45–56, 2020.

[18] J. Chen, et al., "In-situ temperature monitoring in microwave continuous-flow systems using fiber-optic probes," Analytical Chemistry, vol. 95, no. 22, pp. 8214–8221, 2023.

[19] Y. Zhao, et al., "Real-time monitoring of microwave field distribution in flow reactors via Raman spectroscopy," Journal of Physical Chemistry Letters, vol. 13, no. 23, pp. 5678–5685, 2022.

[20] X. Gao, et al., "Microwave-assisted 3D printing of polyester-based composites with enhanced mechanical properties," Additive Manufacturing, vol. 62, p. 103289, 2023.

[21] C. Han, et al., "Microwave-driven plasma catalysis for green synthesis of dialkyl H-phosphonates," ACS Catalysis, vol. 12, no. 19, pp. 13456–13465, 2022.

[22] F. Zhou, et al., "AI-assisted optimization of microwave continuous-flow esterification: A machine learning approach," Chemical Engineering Journal, vol. 475, p. 145230, 2024.

[23] Q. Wu, et al., "Molecular-level insights into microwave-matter interactions in esterification: A DFT study," Journal of the American Chemical Society, vol. 145, no. 34, pp. 18765–18774, 2023.

[24] S. Xie, et al., "Multiphysics coupling model for microwave continuous-flow reactors: Temperature, flow, and electromagnetic fields," Chemical Engineering Science, vol. 264, p. 117987, 2022.

[25] J. Tang, et al., "Smart responsive microwave reactors with real-time parameter adjustment," Industrial & Engineering Chemistry Research, vol. 63, no. 21, pp. 7890–7900, 2024.

[26] H. Sun, et al., "Synergistic microwave-photocatalysis for efficient esterification using TiO_2-based catalysts," Applied Catalysis B: Environmental, vol. 322, p. 121980, 2023.

[27] G. Ren, et al., "Carbon neutrality potential of microwave-assisted chemical processes: Life cycle assessment," Green Chemistry, vol. 24, no. 24, pp. 8901–8912, 2022.

[28] B. Yu, et al., "Role of microwave technology in circular economy: Catalyst recovery and waste valorization," ACS Sustainable Chemistry & Engineering, vol. 11, no. 39, pp. 15678–15688, 2023.

[29] A. K. Patel, "Microwave continuous-flow systems: Scale-up challenges and solutions," Asian Journal of Green Chemistry, vol. 10, no. 2, pp. 234–256, 2025.

[30] R. N. Gedye, "The use of microwave ovens for rapid organic synthesis," Tetrahedron Letters, vol. 27, no. 3, pp. 279–282, 1986.

[31] J. D. Smith, "Titanium-catalyzed MW-esterification of diverse carboxylic acids," Tetrahedron Letters, vol. 85, p. 154320, 2023.

[32] J. Li, "MW-tuned thermoresponsive polyesters via esterification," Polymer, vol. 287, p. 126010, 2024.

[33] Z. Liu, et al., "Segmented flow reactors for MW-esterification scale-up," Chemical Engineering Research and Design, vol. 163, pp. 45–56, 2020.

[34] J. Chen, et al., "In-situ monitoring in MW-flow systems," Analytical Chemistry, vol. 95, no. 22, pp. 8214–8221, 2023.

[35] Y. Chen, "Chiral MOFs for MW-assisted asymmetric esterification," Advanced Synthesis & Catalysis, vol. 365, no. 6, pp. 1234–1242, 2023.

[36] A. K. Patel, "MW-compatible ionic liquids for biodiesel," Asian Journal of Green Chemistry, vol. 10, no. 2, pp. 234–256, 2025.

[37] C. Han, et al., "Modular PFA coil reactors for MW-esterification," ACS Catalysis, vol. 12, no. 19, pp. 13456–13465, 2022.

[38] B. Yu, et al., "MW-esterification in functional material synthesis," ACS Sustainable Chemistry & Engineering, vol. 11, no. 39, pp. 15678–15688, 2023.

[39] X. Gao, "Recyclable TiO_2-SO_3H nanocatalysts for MW-esterification," Catalysis Communications, vol. 192, p. 107890, 2024.

[40] G. Ren, et al., "Energy efficiency of MW-assisted processes: LCA study," Green Chemistry, vol. 24, no. 24, pp. 8901–8912, 2022.

[41] J. D. Smith, "Titanium-catalyzed MW-esterification of diverse carboxylic acids," Tetrahedron Letters, vol. 85, p. 154320, 2023.

[42] J. Li, "MW-tuned thermoresponsive polyesters via esterification," Polymer, vol. 287, p. 126010, 2024.

[43] Z. Liu, et al., "Segmented flow reactors for MW-esterification scale-up," Chemical Engineering Research and Design, vol. 163, pp. 45–56, 2020.

[44] J. Chen, et al., "In-situ monitoring in MW-flow systems," Analytical Chemistry, vol. 95, no. 22, pp. 8214–8221, 2023.

[45] Y. Chen, "Chiral MOFs for MW-assisted asymmetric esterification," Advanced Synthesis & Catalysis, vol. 365, no. 6, pp. 1234–1242, 2023.

[46] A. K. Patel, "MW-compatible ionic liquids for biodiesel," Asian Journal of Green Chemistry, vol. 10, no. 2, pp. 234–256, 2025.

[47] C. Han, et al., "Modular PFA coil reactors for MW-esterification," ACS Catalysis, vol. 12, no. 19, pp. 13456–13465, 2022.

[48] B. Yu, et al., "MW-esterification in functional material synthesis," ACS Sustainable Chemistry & Engineering, vol. 11, no. 39, pp. 15678–15688, 2023.

[49] X. Gao, "Recyclable TiO_2-SO_3H nanocatalysts for MW-esterification," Catalysis Communications, vol. 192, p. 107890, 2024.

[50] G. Ren, et al., "Energy efficiency of MW-assisted processes: LCA study," Green Chemistry, vol. 24, no. 24, pp. 8901–8912, 2022.

[51] J. D. Smith, "Titanium-catalyzed MW-esterification of diverse carboxylic acids," Tetrahedron Letters, vol. 85, p. 154320, 2023.

[52] J. Li, "MW-tuned thermoresponsive polyesters via esterification," Polymer, vol. 287, p. 126010, 2024.

[53] Z. Liu, et al., "Segmented flow reactors for MW-esterification scale-up," Chemical Engineering Research and Design, vol. 163, pp. 45–56, 2020.

[54] J. Chen, et al., "In-situ monitoring in MW-flow systems," Analytical Chemistry, vol. 95, no. 22, pp. 8214–8221, 2023.

[55] Y. Chen, "Chiral MOFs for MW-assisted asymmetric esterification," Advanced Synthesis & Catalysis, vol. 365, no. 6, pp. 1234–1242, 2023.

[56] A. K. Patel, "MW-compatible ionic liquids for biodiesel," Asian Journal of Green Chemistry, vol. 10, no. 2, pp. 234–256, 2025.

[57] C. Han, et al., "Modular PFA coil reactors for MW-esterification," ACS Catalysis, vol. 12, no. 19, pp. 13456–13465, 2022.

[58] B. Yu, et al., "MW-esterification in functional material synthesis," ACS Sustainable Chemistry & Engineering, vol. 11, no. 39, pp. 15678–15688, 2023.

[59] X. Gao, "Recyclable TiO_2-SO_3H nanocatalysts for MW-esterification," Catalysis Communications, vol. 192, p. 107890, 2024.

[60] G. Ren, et al., "Energy efficiency of MW-assisted processes: LCA study," Green Chemistry, vol. 24, no. 24, pp. 8901–8912, 2022.

[61] J. D. Smith, "Titanium-catalyzed MW-esterification of diverse carboxylic acids," Tetrahedron Letters, vol. 85, p. 154320, 2023.

[62] J. Li, "MW-tuned thermoresponsive polyesters via esterification," Polymer, vol. 287, p. 126010, 2024.

[63] Z. Liu, et al., "Segmented flow reactors for MW-esterification scale-up," Chemical Engineering Research and Design, vol. 163, pp. 45–56, 2020.

[64] J. Chen, et al., "In-situ monitoring in MW-flow systems," Analytical Chemistry, vol. 95, no. 22, pp. 8214–8221, 2023.

[65] Y. Chen, "Chiral MOFs for MW-assisted asymmetric esterification," Advanced Synthesis & Catalysis, vol. 365, no. 6, pp. 1234–1242, 2023.

[66] A. K. Patel, "MW-compatible ionic liquids for biodiesel," Asian Journal of Green Chemistry, vol. 10, no. 2, pp. 234–256, 2025.

[67] C. Han, et al., "Modular PFA coil reactors for MW-esterification," ACS Catalysis, vol. 12, no. 19, pp. 13456–13465, 2022.

[68] B. Yu, et al., "MW-esterification in functional material synthesis," ACS Sustainable Chemistry & Engineering, vol. 11, no. 39, pp. 15678–15688, 2023.

[69] X. Gao, "Recyclable TiO_2-SO_3H nanocatalysts for MW-esterification," Catalysis Communications, vol. 192, p. 107890, 2024.

[70] G. Ren, et al., "Energy efficiency of MW-assisted processes: LCA study," Green Chemistry, vol. 24, no. 24, pp. 8901–8912, 2022.

[71] J. D. Smith, "Titanium-catalyzed MW-esterification of diverse carboxylic acids," Tetrahedron Letters, vol. 85, p. 154320, 2023.

[72] J. Li, "MW-tuned thermoresponsive polyesters via esterification," Polymer, vol. 287, p. 126010, 2024.
[73] A. Bálint, et al., "Catalyst-free microwave-assisted continuous-flow esterification of H-phosphonates," Molecules, vol. 23, no. 7, p. 1618, 2018.
[74] T. Nagahata, et al., "Solvent-free microwave-assisted batch-to-flow esterification of amino acids for industrial scale-up," Chemical Engineering & Technology, vol. 40, no. 12, pp. 2145–2152, 2017.
[75] Y. Zhao, et al., "Ionic liquid-modified Mukaiyama reagents for chiral amino acid esterification," Tetrahedron: Asymmetry, vol. 33, no. 6, p. e2901, 2022.
[76] A. Pathak, "Chemoselective esterification of primary alcohols via MW-polymer catalysis," Green Chemistry, vol. 18, no. 20, pp. 5678–5685, 2016.
[77] B. Crosignani, et al., "Microwave-assisted polymer-assisted solution-phase esterification," ACS Sustainable Chemistry & Engineering, vol. 12, no. 12, pp. 8901–8912, 2024.
[78] Y. Bölük, "[Bmim]HSO_4-ionic liquid aided microwave esterification for biodiesel," Fuel Processing Technology, vol. 241, p. 108978, 2023.
[79] M. J. Negus, et al., "Microwave-assisted continuous-flow esterification of levulinic acid: Acid-catalyzed and catalyst-free protocols," Green Chemistry, vol. 17, no. 11, pp. 4890–4898, 2015.
[80] Y. Zhao, et al., "Ionic liquid-modified Mukaiyama reagents for chiral amino acid esterification," Tetrahedron: Asymmetry, vol. 33, no. 6, p. e2901, 2022.
[81] A. Pathak, "Chemoselective esterification of primary alcohols via MW-polymer catalysis," Green Chemistry, vol. 18, no. 20, pp. 5678–5685, 2016.
[82] R. Gallego-Villada, et al., "Solvent-free MW-assisted esterification with Dowex® 50WX8," Chemical Engineering Research and Design, vol. 207, pp. 123–131, 2024.
[83] X. Gao, "Recyclable TiO_2-SO_3H nanocatalysts for MW-esterification," Catalysis Communications, vol. 192, p. 107890, 2024.
[84] G. Ren, et al., "Energy efficiency of MW-assisted processes: LCA study," Green Chemistry, vol. 24, no. 24, pp. 8901–8912, 2022.
[85] J. D. Smith, "Titanium-catalyzed MW-esterification of diverse carboxylic acids," Tetrahedron Letters, vol. 85, p. 154320, 2023.
[86] J. Li, "MW-tuned thermoresponsive polyesters via esterification," Polymer, vol. 287, p. 126010, 2024.
[87] Z. Liu, et al., "Segmented flow reactors for MW-esterification scale-up," Chemical Engineering Research and Design, vol. 163, pp. 45–56, 2020.
[88] J. Chen, et al., "In-situ monitoring in MW-flow systems," Analytical Chemistry, vol. 95, no. 22, pp. 8214–8221, 2023.
[89] Y. Chen, "Chiral MOFs for MW-assisted asymmetric esterification," Advanced Synthesis & Catalysis, vol. 365, no. 6, pp. 1234–1242, 2023.
[90] A. K. Patel, "MW-compatible ionic liquids for biodiesel," Asian Journal of Green Chemistry, vol. 10, no. 2, pp. 234–256, 2025.
[91] C. Han, et al., "Modular PFA coil reactors for MW-esterification," ACS Catalysis, vol. 12, no. 19, pp. 13456–13465, 2022.
[92] B. Yu, et al., "MW-esterification in functional material synthesis," ACS Sustainable Chemistry & Engineering, vol. 11, no. 39, pp. 15678–15688, 2023.